Influence of slope on smoke control in tunnel fires

Ying Zhen Li

Influence of slope on smoke control in tunnel fires

Ying Zhen Li

Abstract

Influence of slope on smoke control in tunnel fires

A series of tests was carried out in a model scale tunnel to investigate the influence of downhill and uphill slopes on smoke control in longitudinally ventilated tunnels. The experimental study considered various fire sizes, from small to large fires, and various slopes, from -20 % (uphill) to 20 % (downhill). Further, a series of simulations of full scale tunnel fires were conducted to verify the findings.

Key words: critical velocity, backlayering length, tunnel, slope

Content

Preface

Summary

A total of 46 tests were carried out in a 1:15 model scale tunnel with various slopes to investigate the influence of downhill and uphill slopes on smoke control in longitudinally ventilated tunnels. The experimental study considered various fire sizes, from small to large fires, and various slopes, from -20 % (uphill) to 20 % (downhill). Further, a series of simulations were conducted to verify the findings in full scale tunnels. A positive slope refers to a tunnel with longitudinal flow blown towards the downhill side and vice versa.

The main findings are summarized below:

(1) Experimental data for downhill slopes ($s \geq 0$) within a range of 0 % – 20 % show that the critical velocity can be well correlated with the downhill slope by Eq. (3):

$$\frac{u_c}{u_c(0)} = 1 + 0.011\,\mathrm{s} \tag{3}$$

where *s* refers to downhill slope ($s \geq 0$).

(2) Experimental data for uphill slopes ($s < 0$) within a range of -20 % – 0 % show that the critical velocity can be well correlated with the uphill slope by Eq. (5):

$$\frac{u_c}{u_c(0)} = 1 + 0.015\,\mathrm{s} \tag{5}$$

where *s* refers to uphill slope ($s < 0$).

(3) For an uphill tunnel, the backlayering length become less sensitive to the variation of tunnel velocity, and there is an upper limit for backlayeirng length, which can be approximately estimated by the following equation:

$$L_{b,\max} = \frac{H_{ef}}{|s|} \tag{6}$$

where H_{ef} is the ceiling height above the bottom of the fire source, i.e. the distance between the bottom of the fire source and the ceiling at a tunnel cross section. If the fire source is on the floor, H_{ef} quals tunnel height *H*.

(4) The previous equation for critical velocity, Eq. (1), correlates well with the test data for the horizontal tunnel. The previous equation for backlayeirng length, Eq. (2), correlates reasonably well with the test data for horizontal tunnel and downhill tunnels, but to make a conservative estimation of the backlayering length, a constant of 25 might be used instead of 18.5 in Eq. (2). It should be kept in mind that the backlayering length for uphill tunnels become less sensitive to the variation of tunnel velocity.

(5) Numerical simulations of full scale tunnels with various cross sections, fire sizes and slopes, confirm the above findings.

© RISE Research Institutes of Sweden

6

1 Introduction

Both the need for fast transportation and the urbanization stimulates tunnel construction, and the number of tunnels is continuously increasing. Smoke control is one of the key issues for any tunnel fire safety design. Tunnels generally have certain slopes, however, the influences of slope on the two most important parameters for smoke control, i.e. the critical velocity and the backlayering length, are uncertain. There have been some studies on the influence of slope on the critical velocity, but the results vary significantly due to inappropriate experimental methods. Further, there is a lack of study on the influence of slope on backlayering length. There is a clear need to conduct researches on the influence of slope on the critical velocity and backlayering length for smoke control in sloping tunnels, in order to provide guidance for engineering applications in tunnel fire safety design.

The objective of this work is to systematically investigate the influence of slope on control of smoke flows in tunnel fires, by carrying out model scale tunnel fire tests and also by full scale tunnel fire simulations using advanced Computational Fluid Dynamics (CFD). The project aims to establish correlations for smoke control in sloping tunnels and provides guidance for engineering applications.

2   Background and state of the art

Tunnels generally have certain slopes either due to geological conditions (e.g. a height difference between portals, or an underwater tunnel) or specific designs with purposes (e.g. a slope for water drainage). It is known that the chimney effect in a sloping tunnel plays a key role in the ventilation flows [1]. However, how the tunnel slope affects the control of smoke is still uncertain, although such information is needed in almost every tunnel project.

Smoke control is of the utmost importance for evacuation and rescue service in tunnel fires [2]. It is one of the key issues for any tunnel fire safety design. In most modern tunnels, a longitudinal ventilation system is applied, i.e. fresh air flow is supplied from one tunnel portal to create a smoke-free region on the upstream of the fire site. The two most important parameters for smoke control in tunnels with longitudinal ventilation are the critical velocity and the backlayering length.

There have been some studies on influence of slope on the critical velocity but the results vary significantly and there has been no consensus on this. Further, there is a lack of study on the influence of slope on backlayering length. A literature review of the influence of slope on critical velocity and backlayering length is given below.

2.1   Influence of slope on critical velocity

A critical velocity is defined as the minimum longitudinal ventilation velocity to prevent reverse flow of smoke upstream of a fire in the tunnel [2], as shown in Figure 1. The dependence of critical velocity on the heat release rate (Q) in a horizontal tunnel has undergone extensive investigation, e.g. Li et al.'s correlations [3, 4] adopted in the coming NFPA 502 standard (2020). The case in an inclined tunnel, however, has received much less attention.
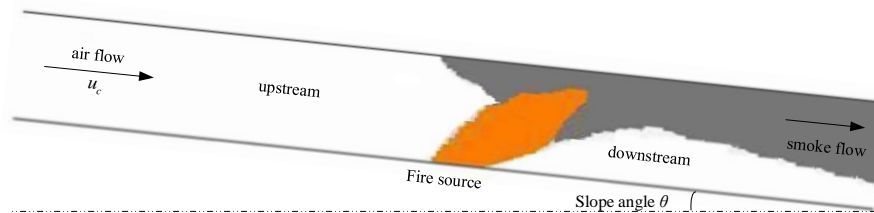

Figure 1. A diagram of critical velocity in a sloping tunnel.

The critical velocity in a sloping tunnel, u_c, is generally correlated with the critical velocity in the corresponding horizontal tunnel, $u_c(0)$, with the following equation:

$$u_c = u_c(0)K_g \qquad (1)$$

where K_g is called grade correction factor that is introduced to consider the influence of slope. Note that tunnel slope, s, can be correlated with the angle, θ, by $s=\tan\theta$. In the following, the slope is defined as positive when the entrance of fresh air is at a higher elevation than the fire source.

Figure 2 gives a comparison of the existing correlations for the grade correction factor, K_g, as a function of tunnel slope. These correlations include the ones proposed by NFPA 502 [5], Atkinson and Wu [6], Ko et al. [7], Yi et al. [8], Chow et al. [9] and Weng et al. [10]. It is clearly shown in Figure 2 that the correlations vary significantly from one to another. The probable reasons for the differences are discussed in the following.

The grade correction factor for the present NFPA 502 (a widely adopted standard worldwide) is derived from the work of Bakke & Leach [11], who studied methane layer propagation in sloping tunnels. Grant et al. [12] commented that "However, the magnitude of the density difference, and the nature of the source of the buoyant flow are very different in these two cases. It is by no means certain that gradient can be represented in such a simple manner, nor even that Bakke & Leach's data are relevant to ventilated tunnel".

Atkinson and Wu [6] used water sprays to cool down the external side of the tunnel model at the fire site, which reduced the convective heat release rate, thus reducing the critical velocity. Such use of water sprays is contradictory to the scaling laws [13]. How this measure affects the results for tunnels with various slopes is uncertain.

Ko et al. [7], Yi et al. [8], Chow et al. [9] and Weng et al. [10] conducted experiments with small liquid pool fires, where the burning rate (fire size) is significantly affected by the ventilation and tunnel structure, and also varies significantly with time [14]. This indicates that the increase in critical velocity in a sloping tunnel is not only due to the slope but also the changed fire size. However, all of these authors ignored the differences in the fire size and directly considered the ratio of the critical velocity in a sloping tunnel to that in a horizontal tunnel as the grade correction factor. Therefore, the uncertainties related to these tests are expected to be rather high.

Further, in some studies, the range of slopes tested was narrow and the tunnel was very short in comparison to the tunnel cross section. Yi et al. [8] only investigated the influence of slope in a range of -3% and 3%, and Weng et al. [10] only tested the slope in a range of 0 to 1%. In Chow et al.'s tests [9], the fire in the tunnel (1 m high and 1.5 m wide) was around 5.5 m from the upstream portal, outside of which an axial fan was placed. The dimensionless length between the fire and the portal with the fan is around 3.7 – 5. The air flow supplied by the axial fan was probably not be fully developed at the fire site, which can significantly affect the results.

The issues mentioned above are considered to be responsible for the difference in Figure 2. Clearly, the relatively high uncertainties related to these experimental data cause problems in drawing any concrete conclusion on the influence of slope on critical velocity. There is a need to carry out tests more scientifically to investigate this issue, in order to provide guidance for engineering applications.
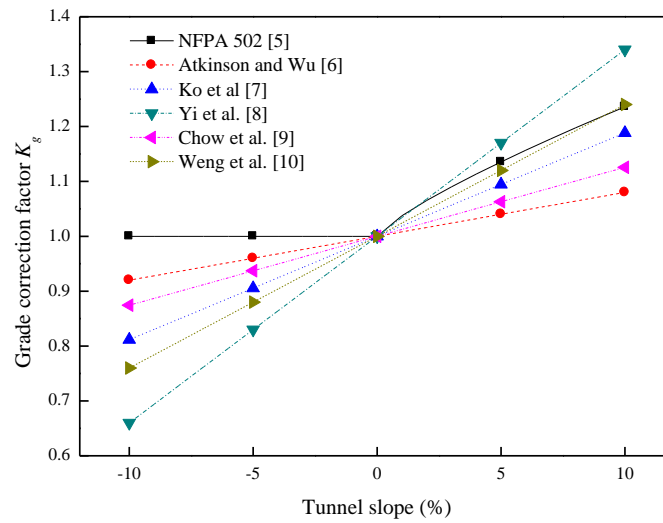
Figure 2. Existing correlations for grade factor K_g vs. tunnel slope in percentage.

2.2 Influence of slope on backlayering length

The backlayering length, L_b, is defined as the length of the smoke backlayering upstream of the fire when the ventilation velocity, u_o, is lower than the critical velocity [2], as shown in Figure 3. In a longitudinally ventilated tunnel, a fresh air flow with a velocity not lower than the critical velocity at the designed fire size is created to prevent smoke backlayering. However, smoke stratification downstream of the fire may not persist as the ventilation velocity is too high. For this reason, a velocity slightly less than the critical velocity may be applied to allow backlayering of a short length. This is also beneficial to reduce the tunnel ventilation capacity.
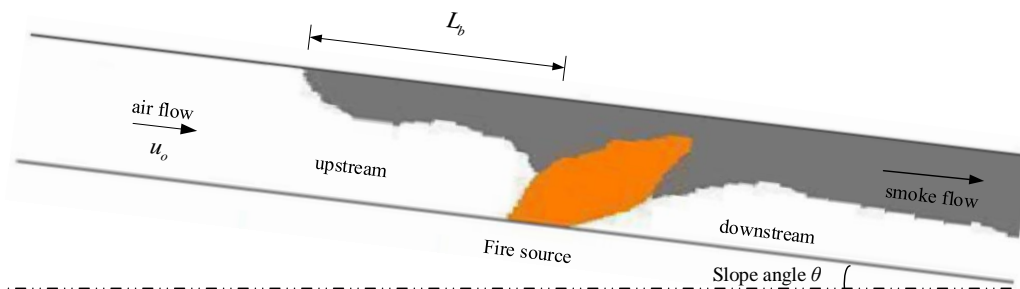
Figure 3. A schematic diagram of backlayering in a tunnel fire.

Thomas [15] gave a simple one dimensional theoretical analysis of the backlayering length in case of a fire in a longitudinally ventilated tunnel. He correlated the backlayering length with the Froude Number.

Li et al. [3] carried out two series of tests in model scale tunnels and found that the backlayering length increases with the fire size for small fires and is nearly independent of fire size and dependent only on the ventilation velocity for larger fires. It was found that the relationship

between the ratio of longitudinal ventilation velocity to critical velocity and the dimensionless backlayering length, L_b^*, follows an logarithmic correlation [3]:

$$L_b^* = \frac{L_b}{H} = 18.5\ln(u_c / u_o) \qquad (2)$$

However, how the slope affects the backlayering length is unknown. Also, how long the backlayering is allowed in such scenarios is also uncertain.

2.3   A short summary

Smoke control is one of the key issues for any tunnel fire safety design. Tunnels generally have certain slopes. However, the influences of slope on the two most important parameters for smoke control, i.e. the critical velocity and the backlayering length, are uncertain. There have been some studies on influence of slope on the critical velocity, but the results vary significantly probably due to inappropriate experimental methods and there has been no consensus on this. Further, there is a lack of study on the influence of slope on backlayering length.

There is a clear need to conduct research on the influence of slopes on the critical velocity and backlayering length in tunnel fires, in order to provide guidance for engineering applications in tunnel fire safety design. This work aims to establish correlations for the influence of tunnel slope on the critical velocity and backlayering length and provides guidance for practical applications. The knowledge can directly be used for design of ventilation systems in tunnels with various slopes and support in new regulations on tunnel safety.

3 Simple theoretical considerations

It is known that in a tunnel with natural ventilation (no ventilation), the fire plume develops in a way similar to that in an enclosure or corridor, see Figure 4. Imagine that an air flow is suddenly blown into the tunnel from left to right. If the momentum of the air flow (or air velocity) is high enough, the smoke at point 2 could be all blown back to the downstream side.
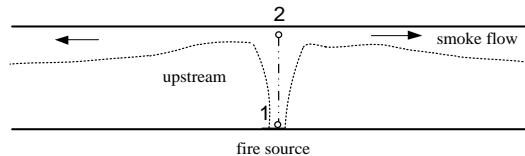

Figure 4. A schematic drawing of smoke flow under natural ventilation for a horizontal tunnel

For a downhill tunnel with a longitudinal velocity of 0 m/s, the flow is shown in Figure 5, not as symmetrical as shown in Figure 4. After impinging on the ceiling, a greater portion of the vertical smoke flow will flow towards the uphill side, resulting a thicker smoke layer and a higher thermal pressure, $\Delta \rho g h \cos \theta$ (Note that this term is closely the same as $\Delta \rho g h$ for slope less than 20 %). Besides, there is an additional buoyancy force directly acting to the flow at the x axis, i.e. $\Delta \rho g h \sin \theta$. Further, it can be expected that the smoke flow that flows towards the downhill side will turn back after a certain distance due to the heat loss, entrainment and the additional buoyancy force towards upstream. All these factors indicate that the smoke flow in such a downhill tunnel is more difficult to be controlled (a greater longitudinal velocity is required), compared to that in a horizontal tunnel, while the smoke control becomes easier in an uphill tunnel. The additional buoyancy force acting to the flow at the x axis, i.e. $\Delta \rho g h \sin \theta$, plays a key role in the influence of slope on smoke control. Note that for tunnel slope less than 20 %, the term $\sin \theta$ is closely the same as the tunnel slope, $\tan \theta$, and thus in the following sections, the tunnel slope is directly investigated as the key parameter.
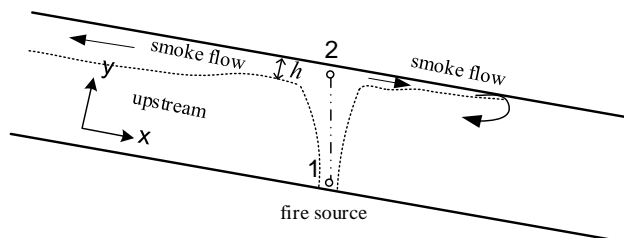

Figure 5. A schematic drawing of smoke flow for a sloped tunnel with velocity of 0 m/s at the initial fire development stage.

4 Froude scaling

The Froude scaling technique has been applied in this work. It is in most cases not necessary to preserve all the terms obtained by scaling theory simultaneously and only the terms that are most important and most related to the study are preserved. The Froude scaling has been used widely in researches on enclosure fires and tunnel fires. Previous work showed that there is a good agreement between model scale and large scale test results on many focused issues [3, 16-18].

The model tunnel was built in a scale of 1:15, which means that the size of the tunnel is scaled geometrically according to this ratio. The scaling of other variables such as the heat release rate, flow rates and the water flow rate can be seen in Table 1. General information about the Froude scaling can be found in the literature [19].

The radiation is not explicitly scaled. However, the previous work on enclosure fires [13] indicates that the radiation can be relatively well scaled if appropriate enclosure materials are applied in model scales.

For laminar flows, the viscous terms play significant roles in flows and heat transfers. Unfortunately, these terms cannot be scaled in the Froude scaling. However, for turbulent flows, the turbulent viscous terms can be well scaled [19]. This indicates that the Froude scaling works better in turbulent flows. Therefore, while carrying out model scale tests we should try to have turbulent flows in model scales.

Table 1. A list of scaling correlations for the model tunnel.

Type of unit	Scaling correlations[*]
Heat Release Rate (HRR) $\dot{Q}$ (kW)	$\dot{Q}_M / \dot{Q}_F = (l_M / l_F)^{5/2}$
Mass flow $\dot{m}$ (m³/s)	$\dot{m}_M / \dot{m}_F = (l_M / l_F)^{5/2}$
Velocity u (m/s)	$u_M / u_F = (l_M / l_F)^{1/2}$
Time t (s)	$t_M / t_F = (l_M / l_F)^{1/2}$
Gas concentration Y^*	$Y_M / Y_F = 1$
Temperature T (K)	$T_F = T_M$
Thermal inertia $k\rho c$ (kW²·s·m⁻⁴·K⁻²)	$(k\rho c)_{s,M} / (k\rho c)_{s,F} \propto (l_M / l_F)^{3/2}$
Thickness δ (m)	$(k/\delta)_{s,M} / (k/\delta)_{s,F} \propto (l_M / l_F)^{1/2}$

L is the length scale (m). Index M is related to the model scale and index F to full scale (L_M=1 and L_F=15 in our case).
[*]Assume the ratio of heat of combustion $\Delta H_{c,M} = \Delta H_{c,F}$.

5 Model scale tunnel tests

5.1 Tunnel model

A total of 46 tests were carried out in a 1:15 model scale tunnel, see Figure 7. The Froude scaling technique was applied in this work. The model tunnel was around 0.33 m high, 0.52 m wide and 9 m long, corresponding to a 5 m high, 7.8 m wide and 135 m long tunnel at full scale. The tunnel slope was varied in a range of -20 % to 20 %, including -20%, -10%, -6%, 0%, 3%, 6%, 10%, 15% and 20%. To facilitate the adjustment of tunnel slope, the tunnel was built on an adjustable platform. Promatect H boards are used as tunnel structure. The tunnel sections were made of 10 mm thick boards but the ceiling of the last section TS3 with fire was made of 20 mm thick boards.

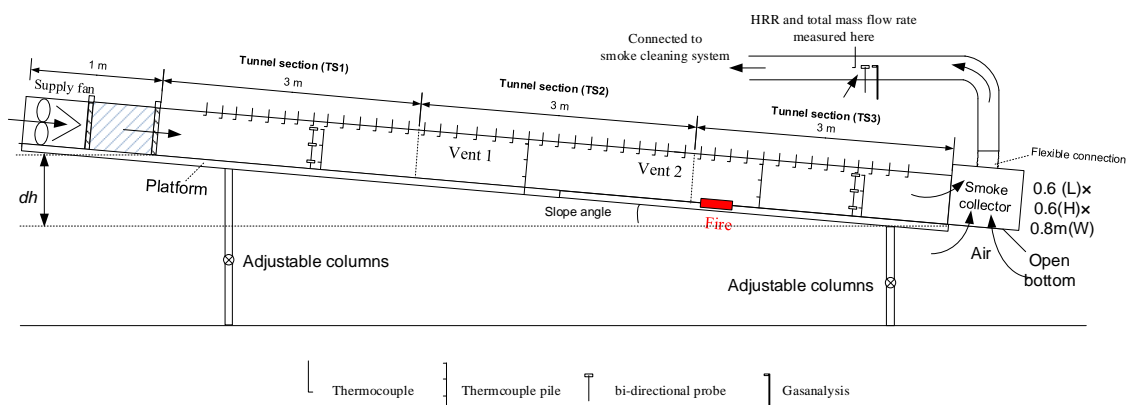*Figure 6. A photo of the model scale tunnel with adjustable slopes (20 % downhill slope).*

Figure 7. Schematic drawing of the model scale tunnel with adjustable slopes (downhill slopes).
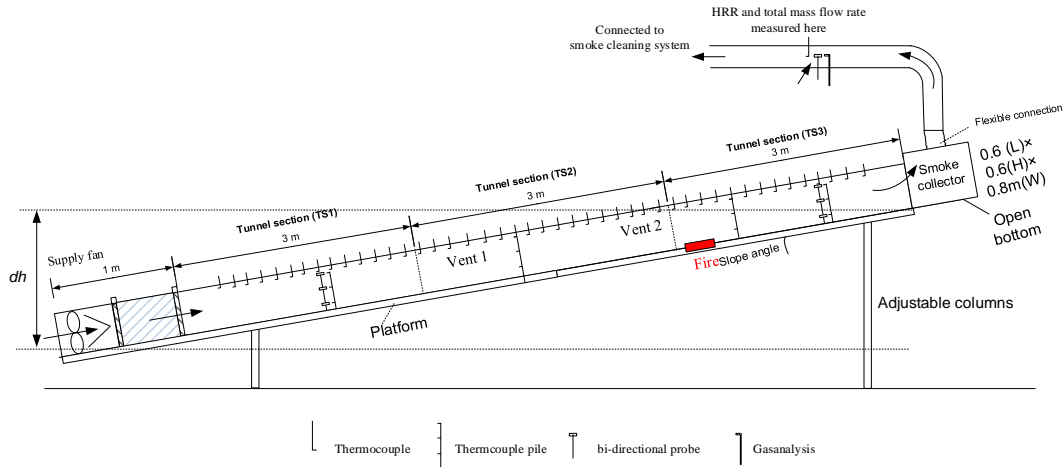
Figure 8. A schematic drawing of the model scale tunnel with adjustable slopes (uphill slopes).

5.2 Ventilation

An around 1 m long fan section was attached to the left tunnel portal to produce a longitudinal flow along the tunnel. The smoke was collected by a smoke collector connected to the right tunnel portal and delivered into an exhaust pipe that is connected to the central smoke cleaning system. A flexible duct was be used to connect the smoke collector and the exhaust pipe to facilitate the change of the tunnel slope. The smoke collector box was 0.6 m long, 0.6 m high and 0.8 m wide (along the tunnel width).

A frequency adjustor was used to control the fan frequency in order to obtain the desired tunnel velocity.

5.3 Fire sources

A gas burner was used as the fire source, as the fire sizes were pre-set and the objectives were not to investigate fire development. This can avoid the problem with changing fire sizes as mentioned in Section 2.1 concerning previous tests with small pool fires. Therefore, in this study, the change of critical velocity and backlayering length in a sloping tunnel will be only due to the influence of slope. In other words, a fair parametric study of the influence of tunnel slope on smoke control is feasible.

A 10cm×10cm×10 cm cubic burner with extension on top with a side width of 3 cm is used. The extended part was on the floor, avoiding leakage from the gap between burner and tunnel floor. The burner surface is set on the floor. Propane was used as the fuel. The fire size tested was in a range of 5 kW – 60 kW, corresponding to full scale 4 MW - 52 MW.
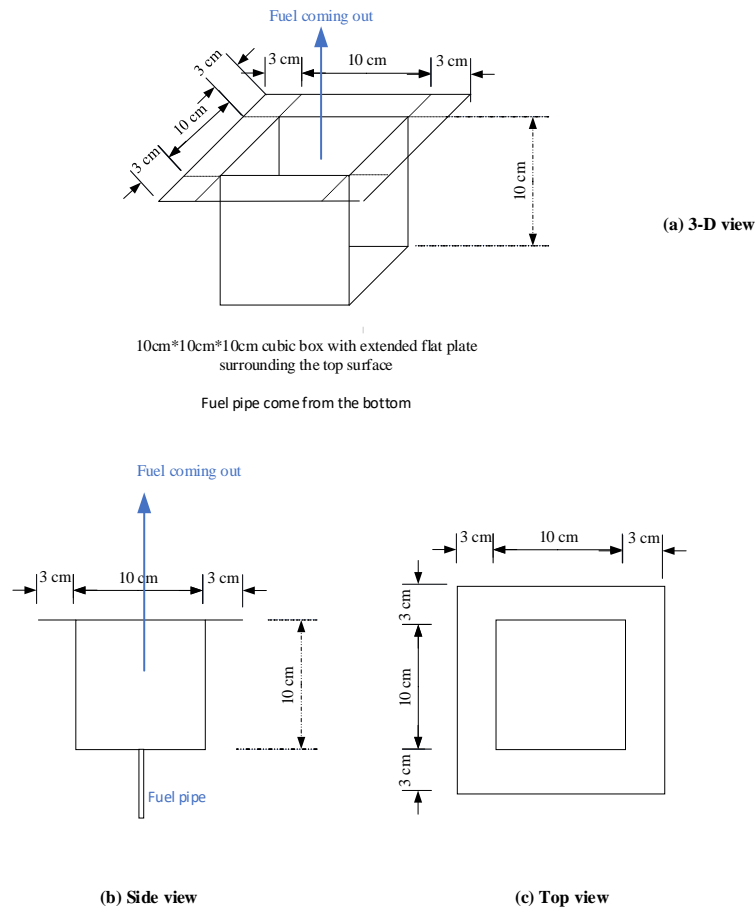
(a) 3-D view

10cm*10cm*10cm cubic box with extended flat plate
surrounding the top surface

Fuel pipe come from the bottom

(b) Side view

(c) Top view

Figure 9. Gas burner with extension part on the top.

5.4 Measurements

Various measurements were made on both sides of the fire source, including thermocouples for temperature measurements, bi-directional pressure probes for velocity measurements and gas analysis for gas concentration measurements (see Figure 10). The numbering of instruments can be found in Appendix A.

Ceiling thermocouples were placed 30 mm below the ceiling to measure temperature in order to identify the location of smoke front, as it is known that at the smoke front, the temperature rapidly drops to value close to ambient temperature. By varying velocities, data for different backlayering lengths can be obtained. By extrapolation of the backlayering length curve, the critical velocity can be obtained. Vertical temperature distributions on the upstream and downstream sides were also measured and could be used to facilitate the analysis of tenability for evacuation.

All ceiling thermocouples were placed at 30 mm below the ceiling (300 mm above floor). The interval between the ceiling thermocouples between -2 m and 0.8 m, 0.2 m between -4.4 m and -2 m, 0.4 m beyond -4.4 m, and 0.4 m between 1.0 m and 2.5 m downstream. "-" means upstream and positive value means downstream.

Two velocity trees were placed, with one at 4.4 m upstream and another at 1.8 m downstream.

Ceiling gas concentrations and velocities were measured 30 mm below the ceiling at three locations, i.e. -1 m, -2 m and -3 m. These measurements are used to estimate how velocity and concentration vary with distance and the entrainment, providing data for future analysis.

The tunnel velocity was estimated based on the velocities measured at Pile D at -4.4 m upstream. If the backlayering is close to or beyond this location, the measurement will not be accurate, and such tests are not of interest. The measured backlayering length of key interest varies within around 3.5 m.
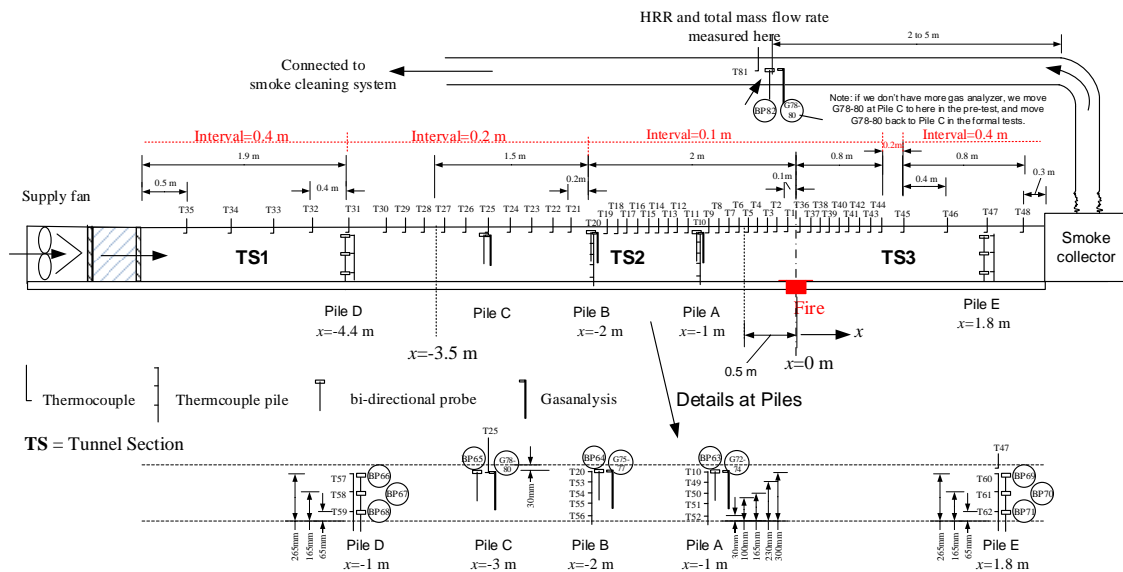

Figure 10. A schematic drawing of the model scale tunnel with adjustable slopes.

6   Test procedure

A total of 46 tests were carried out in a 1:15 model scale tunnel with various slopes, including 40 tests with downhill slopes and 6 tests with uphill slopes.

6.1   Downhill tunnel fire tests

Six series of tests were conducted for downhill tunnels, each having a different slope. A list of these tests is given in Table 1. For example, A name "103" means test series 1 and the 3rd test.

Each test was started with an initial velocity that is slightly lower than the estimated critical velocity, and then the velocity was reduced step by step to allow longer and longer backlayering on the upstream of the fire until the smoke front reaches a location close to Pile D. Minimum four data points were required to plot a graph showing how the backlayering length varies with the velocity. To reduce the uncertainty, the four data points were rather uniformly distributed over the range in each test.

The standard procedure for each test is listed below:
  (1)   Adjust the laboratory smoke exhaust system to the designed value;
  (2)   Adjust the velocity to the designed value;
  (3)   Adjust the gas burner controller to the designed value.
  (4)   Start the recording at t=0 min.
  (5)   Release the gas and ignite the fire at t=1 min.
  (6)   Identify the position of smoke backflow front (upstream) by ceiling temperature distribution and thereafter determine the backlayeirng length, i.e. the distance between the fire center and the smoke front.
  (7)   At t=4 min, reduce the velocity by around 0.06 - 0.08 m/s (this value may vary slightly from case to case), and then check the backlayering length.
  (8)   At t=6 min (2 min later), reduce the velocity by around 0.06 - 0.08 m/s (this value may vary slightly from case to case), and then check the backlayering length.
  (9)   Repeat (8) until the backlayering closely reaches around -3.5 m (close to the velocity measurement upstream Pile D).
  (10) End the test. If less than 4 useful data points were obtained, repeat the whole test with a higher initial value.

The tests were started from horizontal tunnel and then the slope was increased step by step as listed in Table 1.

Before the formal tests, several ventilation tests were conducted to approximately know the relationship between the velocity and the fan frequency. One test with a 10 kW fire was also conducted to compare the velocity measurement in the tunnel and in the exhaust duct.

Table 2. List of tests with downhill slopes.

Test nr	Slope	Fire size
	%	kW
101	0	5
102	0	6.5

103	0	8.3
104	0	9.4
105	0	20
106	0	40
107	0	60
201	3	6.5
202	3	8.3
203	3	9.4
204	3	20
205	3	40
206	3	60
301	6	5
302	6	6.5
303	6	8.3
304	6	9.4
305	6	20
306	6	40
307	6	60
401	10	5
402	10	6.5
403	10	8.3
404	10	9.4
405	10	20
406	10	40
407	10	60
501	15	5
502	15	6.5
503	15	8.3
504	15	9.4
505	15	20
506	15	40
507	15	60
601	20	6.5
602	20	8.3
603	20	9.4
604	20	20
605	20	40
606	20	60

6.2   Uphill tunnel fire tests

Six tests were conducted with uphill slopes. See Table 3. The slopes tested include -6 %, -10 % and -20 % and the fire sizes include 9.4 kW and 40 kW. The minus before slope indicates uphill slope. The test procedure is the same as that described in Section 6.1 for downhill tunnels.

Table 3. List of tests with uphill slopes.

Test nr	Slope	Fire size
	%	kW
701	-6	9.4
702	-6	40
801	-10	9.4
802	-10	40
901	-20	9.4
902	-20	20

# 7 Experimental results and analysis – Downhill tunnels

It is found from the results that the scenarios with uphill slopes and downhill slopes are rather different, and thus they are separated in the following analyses. The data for downhill slopes will be analyzed in this chapter and the data for uphill slopes will be presented in Chapter 8.
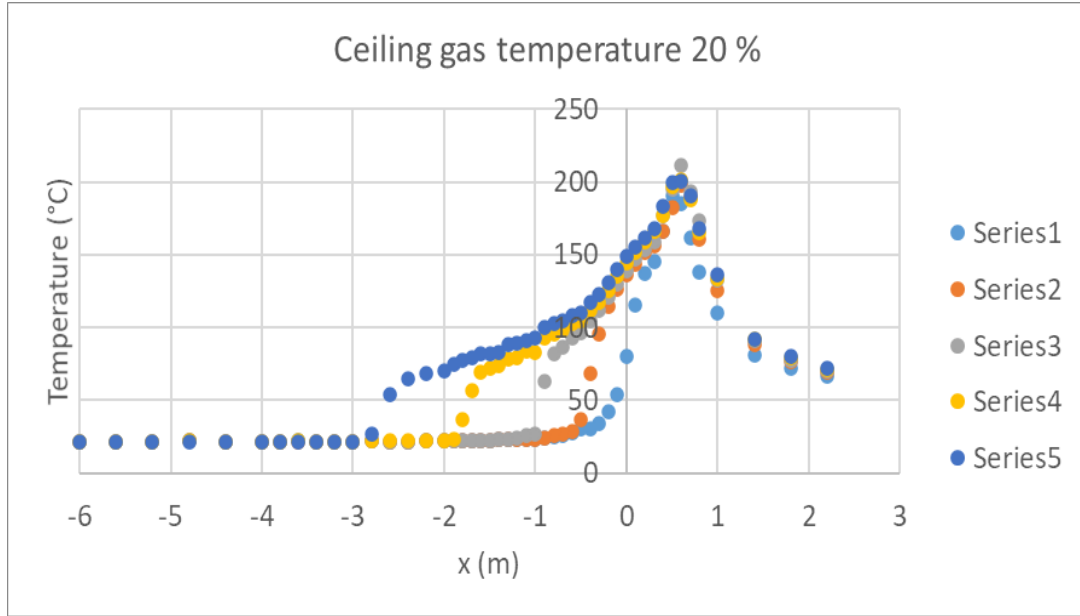
7.1 Gas temperatures

Measured ceiling gas temperatures for 6.5 kW fire in tunnels with 0 % and 20 % are shown in Figure 11. A minus value for x means upstream. It can be seen that with a longer backlayering the ceiling smoke temperature along the tunnel is also higher, both upstream and downstream of the fire.

At the smoke front on the upstream side, the ceiling gas temperature drops rapidly to ambient within a short range, which is typically around 0.2 m or half of the tunnel height. So based on analysis of the ceiling temperature distribution, the locations of the smoke fronts can be determined, which thereafter can be used to determine the critical velocity by plotting the backlayering length curve as a function of the velocity.

Comparing (a) for 0 % and (b) for 20 % shows that for a given backlayeirng length, the ceiling gas temperature for the 20 % sloped tunnel is much lower. Further, it can be noticed that the position of the measured maximum ceiling gas temperature for 20 % is further away from the fire compared to that for 0 %. Both phenomena could be mainly due to the fact that the velocity to obtain a given backlayering length is higher for the 20 % sloped tunnel, which will be further discussed in Section 7.3.
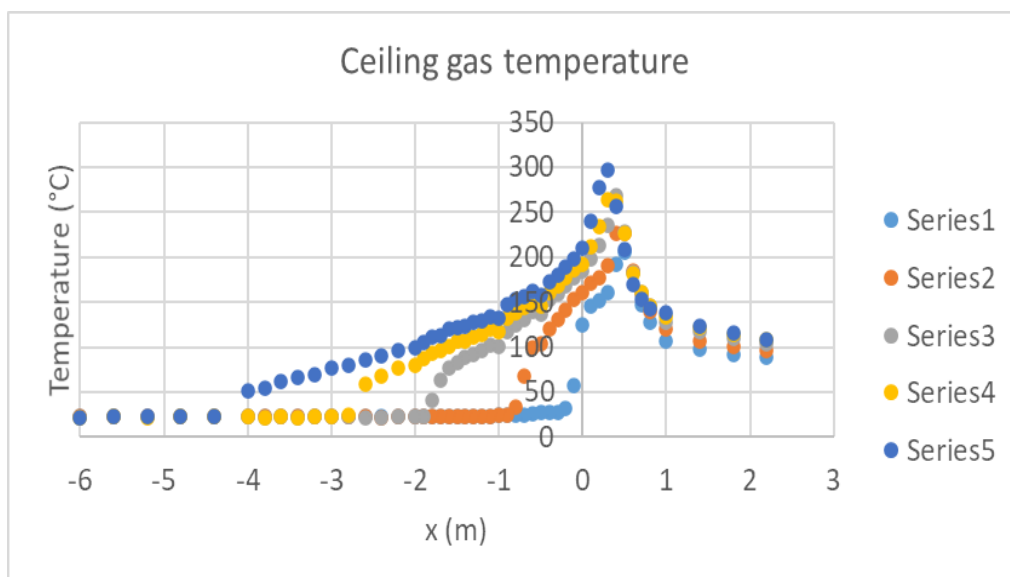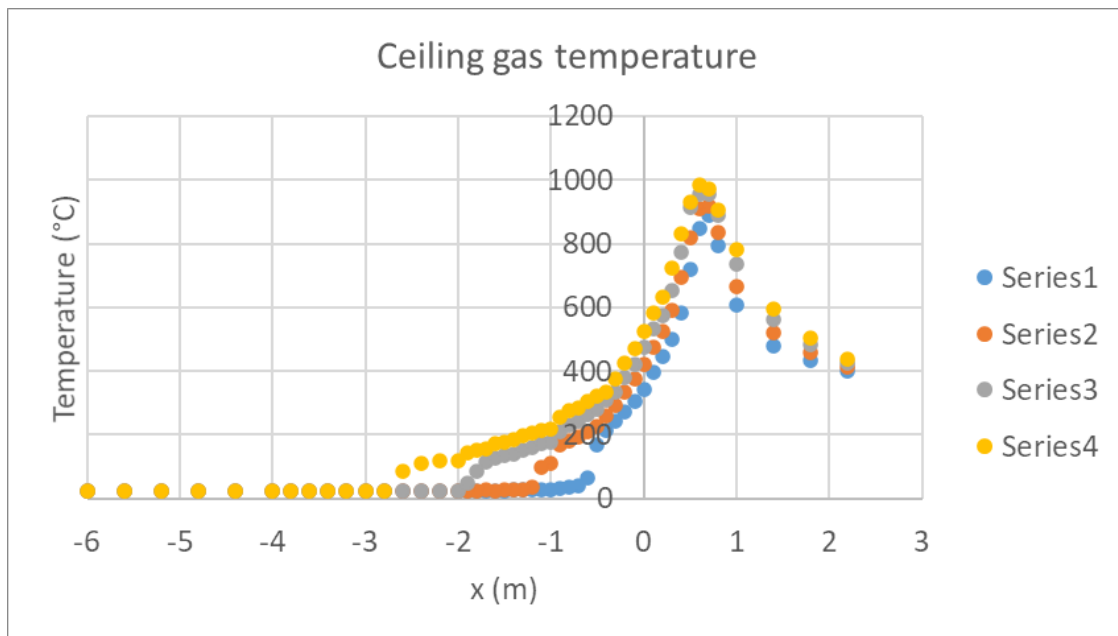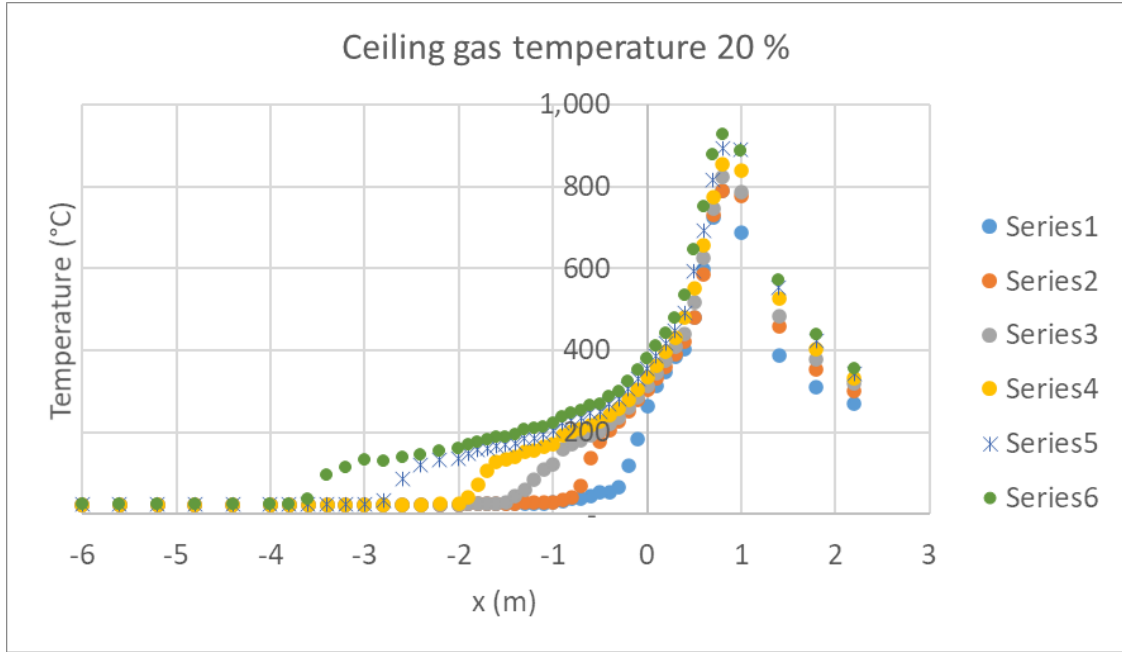

(a) 0 %

(b) 20 %

Figure 11. Comparison of ceiling gas temperatures between 0 % amd 20 % for 6.5 kW fire.

Figure 12 shows the measured ceiling gas temperatures for 60 kW fire in tunnels with 0 % and 20 %. Similar phenomena can be found concerning temperature and position of the maximum temperature. It is interesting to see that the ceiling gas temperature at 1 m (15 m in full scale) for the 60 kW fire (52.3 MW in full scale) and both tunnel slopes is in a range of 200 °C – 250 °C when the backlayering length is within 1.2 m – 3 m (3-10 times tunnel height). This temperature corresponds to an incident heat flux lower than 5 kW/m², indicating that the fire fighters may reach this location. However, the temperature could be higher for a larger fire.

(a) 0 %

(b) 20 %

Figure 12. Comparison of ceiling gas temperatures between 0 % amd 20 % for 60 kW fire.

It could be interesting to compare the dimensionless upstream smoke temperature $\Delta T/\Delta T(x=0)$ to see the variation of temperature with distance for different fire sizes. See Figure 13 for 0% and Figure 14 for 20 % as examples. The temperature ratio decreases slightly more rapidly for the larger fire. Comparing the curves with the same fire size shows that the temperature ratio decays more slowly for a larger tunnel slope.
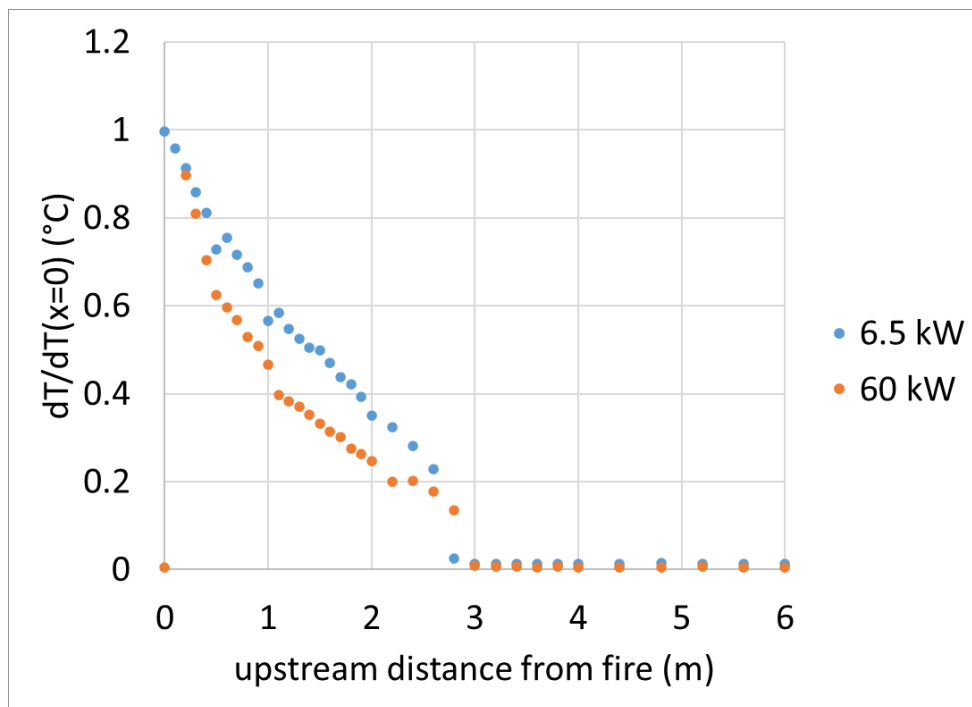

Figure 13. Comparison of ceiling gas temperatures on the upstream side for 6.5 kW and 60 kW fire in tunnel with 0 % slope.
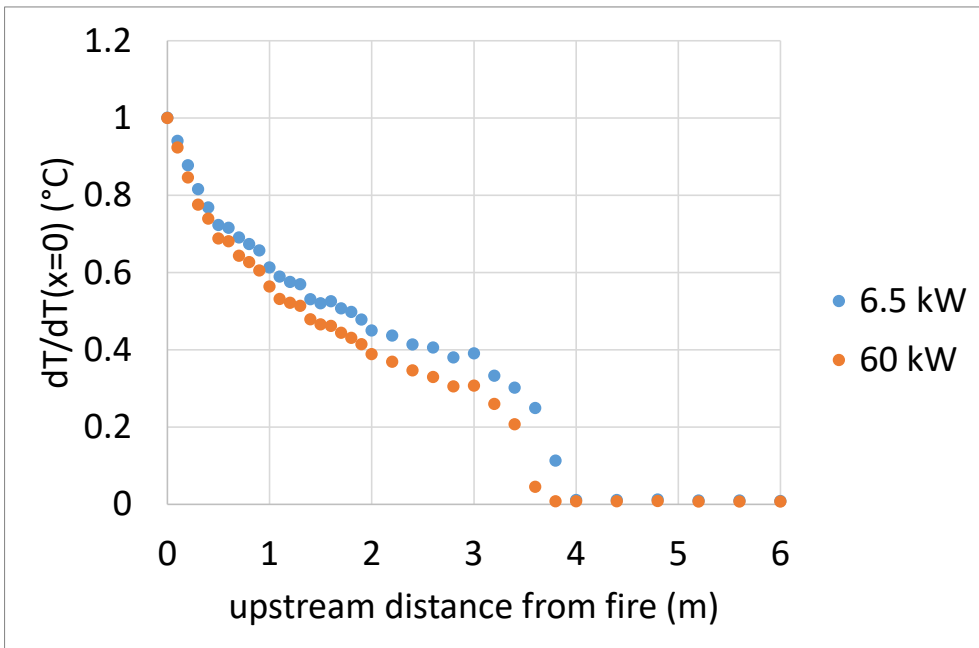
Figure 14. Comparison of ceiling gas temperatures on the upstream side for 6.5 kW and 60 kW fire in tunnel with 20 % downhill slope.

7.2 Critical velocity for downhill tunnels

At first, a comparison of the test data for horizontal tunnel (0 % slope) with the previous data obtained in 2018 for horizontal tunnel [20] and Eq. (1) is made, as shown in Figure 15. It can be seen that there is good agreement among the test data from this study, the test data from the 2018 tests and Eq. (1).

Note that the data for the horizontal tunnel form the basis of the study on the influence of slope on smoke control in the following sections.
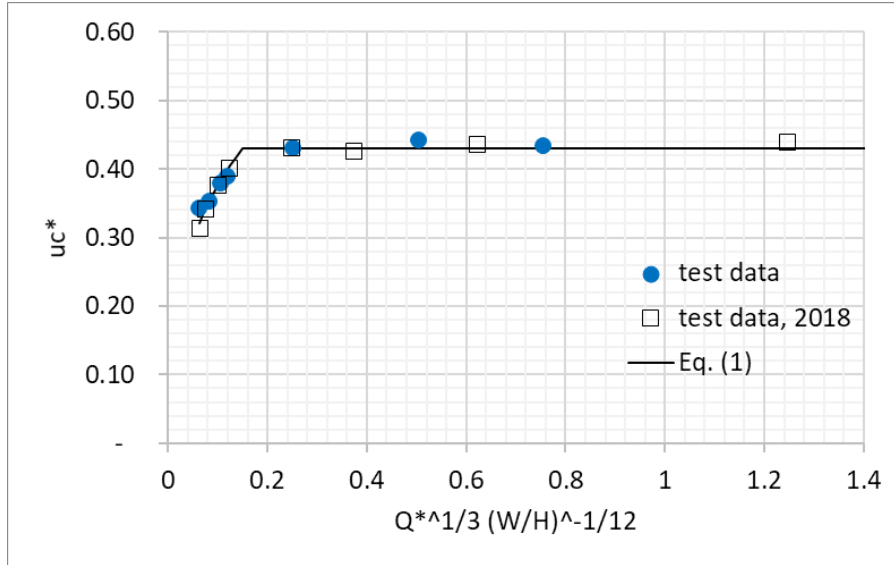
Figure 15. Comparison of test data for critical velocity with Eq. (1).

7.2.1 Influence of fire size and slope

The obtained critical velocities for different slopes (test series 1 – 6) are plotted in Figure 16. It clearly shows that the critical velocity increases with heat release rate lower than 10 kW, and then becomes insensitive to heat release rate higher than 20 kW.

It can also be seen that a greater slope generally corresponds to a greater critical velocity for a given heat release rate, as expected.
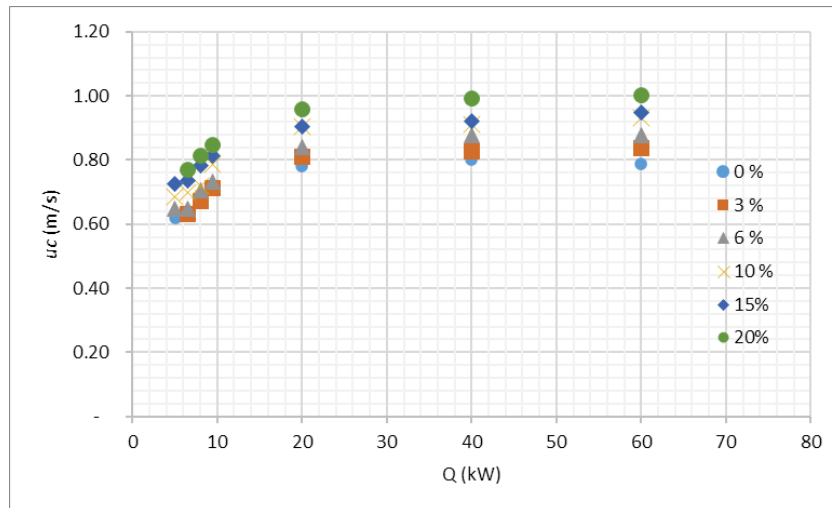

Figure 16. Critical velocity vs heat release rate for downhill tunnels.

To understand the correlation between tunnel slope, heat release rate and critical velocity, we plot the critical velocity ratio $u_c/u_{c,o}$ (i.e. K_g) as a function of slope for each fire size in Figure 17.
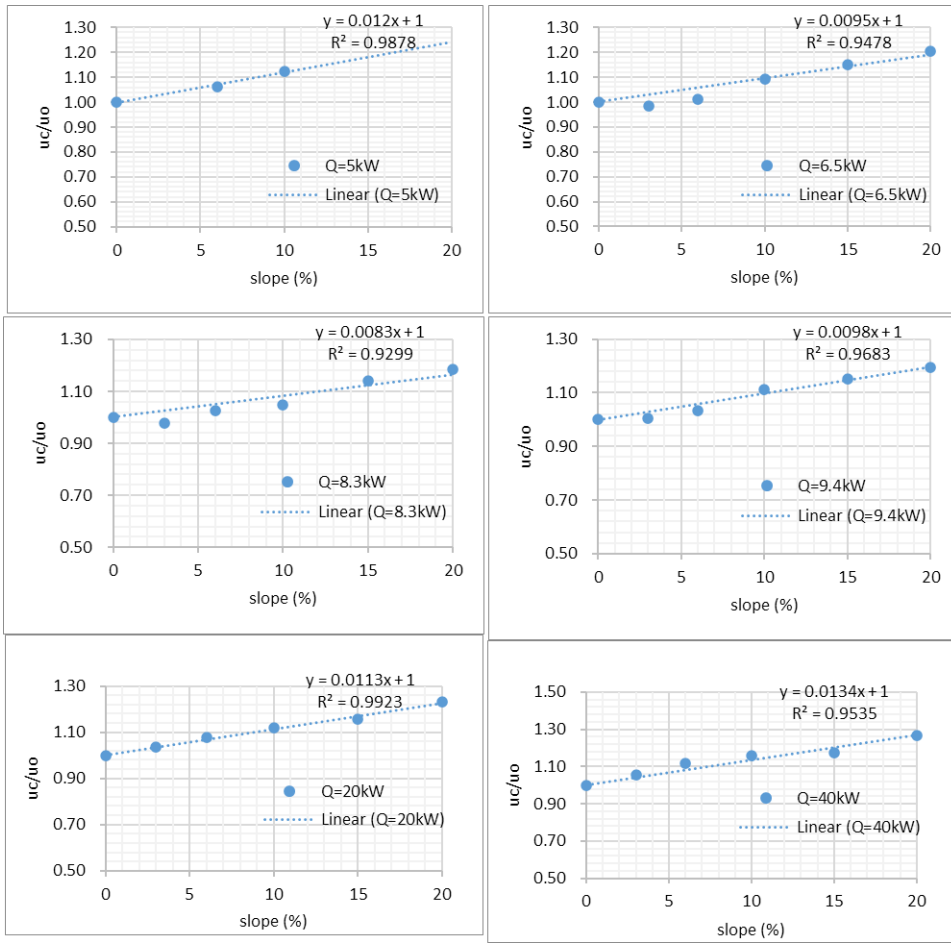
Figure 17. Fitting of critical velocity ratio vs slope for various heat release rates in test series 1 - 6.

In Figure 17, it appears to be that a linear equation well correlates the two parameters, as found in previous research, while the fitting slope varies slightly. The slopes of the fitting correlations are plotted in Figure 18 as a function of heat release rate. The slope of the fitting correlation varies mainly between 0.09 and 0.013. The average slope is around 0.011. From Figure 18, it seems to be that the slopes of the fitting correlations slightly increases with the heat release rate. This effect will be examined in the following part.

Figure 18. The ratio of the critical velocity ratio and slope vs. heat release rates.

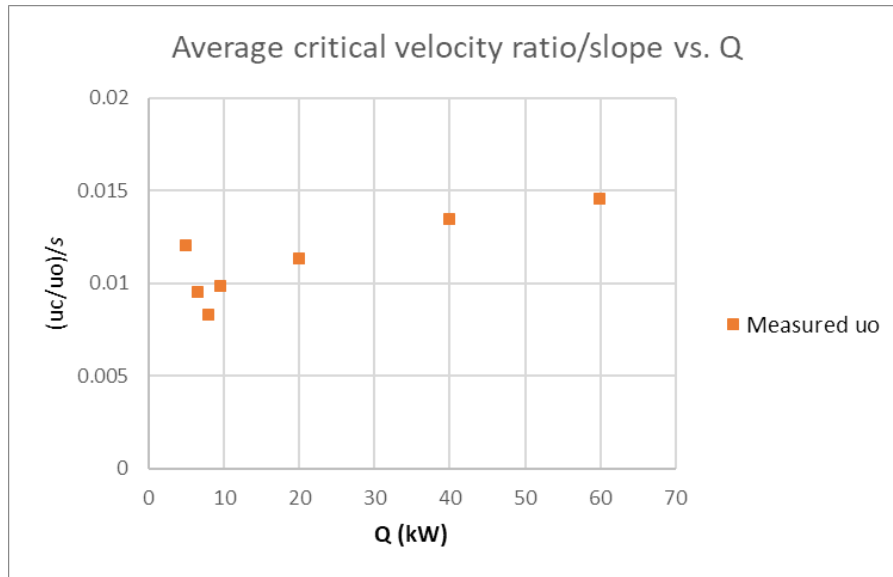In the above analysis of the critical ratio of $u_c/u_{c,o}$, the measured critical velocities at slope=0 % were used. In case of a high uncertainty related to $u_{c,o}$, the critical ratio will also be higher. In other words, if the measured $u_{c,o}$ in one test is far from the real value, all the critical ratios for this heat release rate are influenced. The uncertainty of the critical ratio of $u_c/u_{c,o}$ can be minimized by replacing the measured $u_{c,o}$ with an extrapolated $u_{c,o}$, which can be obtained by extrapolation of all the data for this heat release rate, given that there appears to be a good linear correlation between the critical velocity ratio and the tunnel slope.

The new results are shown in Figure 19. It can be seen that the fluctuation of the critical velocity ratio/slope becomes less while using the extrapolated $u_{c,o}$ as the reference value, indicating lower uncertainties as expected. In reality, the ratio of critical velocity ratio to the fitting slope is closely constant, 0.011. This confirms that the slope effect is insensitive to the heat release rate, and a general linear correlation can be used to reasonably account for the slope effect on critical velocity, regardless of heat release rate.
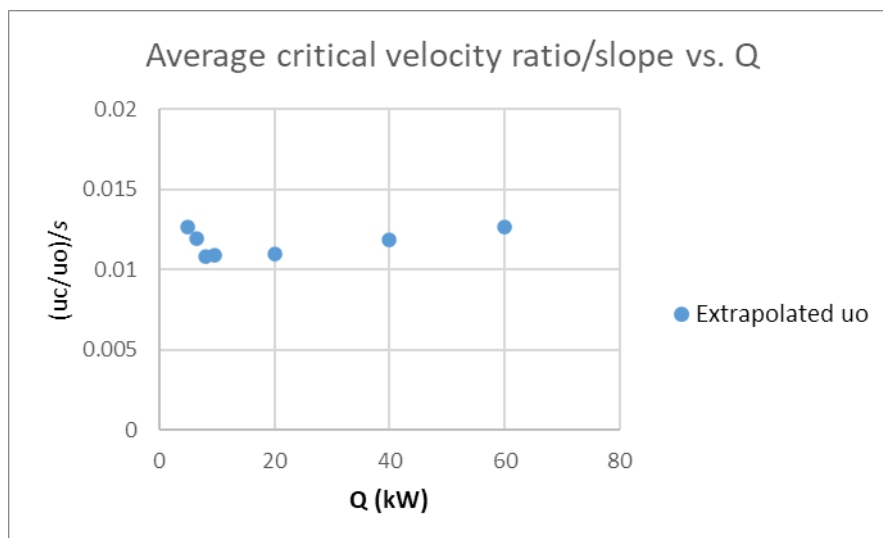

Figure 19. The ratio of the critical velocity ratio and slope vs. heat release rates.

7.2.2 Correlation for critical velocity with slope

The insensitivity of critical velocity ratio to the heat release rate means that the data for various heat release rates can be averaged for a given slope in the following analysis. The averaged data for critical velocity ratio are plotted as a function of slope in Figure 20. It can be seen that the averaged data are well correlated with the following linear correlation:

$$\frac{u_c}{u_c(0)} = 1 + 0.011\text{s} \tag{3}$$

where s is tunnel slope in %. The above equation indicates that if a tunnel has a downhill slope of 10 %, the critical velocity will be increased by 11 % in comparison to the corresponding horizontal tunnel.
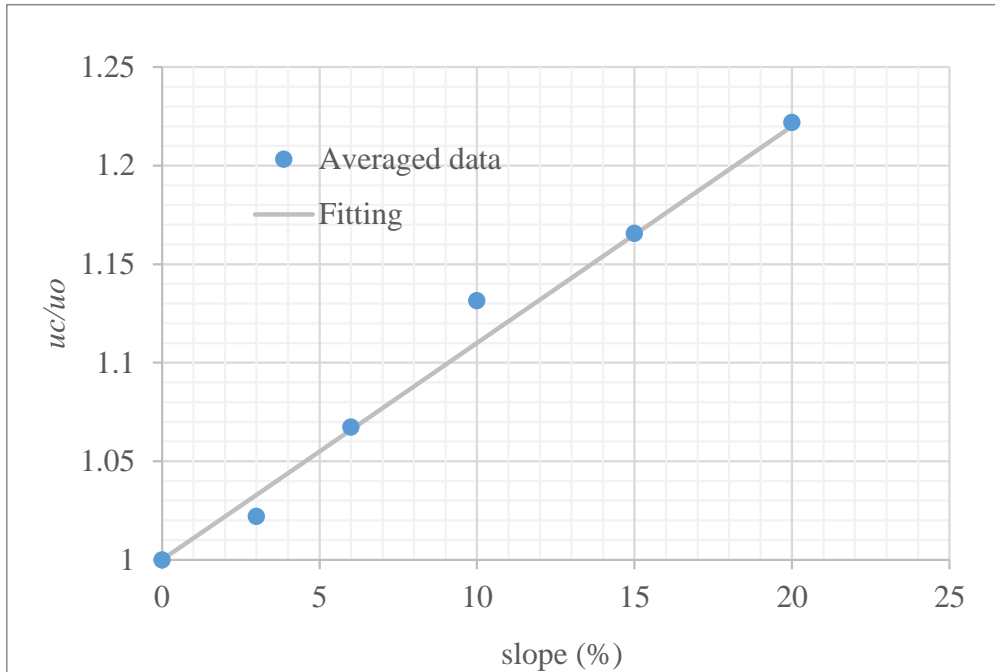
Figure 20. Critical velocity ratio vs slope for various heat release rates.

7.2.3 Comparison with other models in literature

Figure 21 gives a comparison of the test data and the other correlations for the grade correction factor, Kg, as a function of tunnel slope, together with the proposed correlation. It is clearly shown that most of the correlations, e.g. the existing NFPA 502 grade correction equation, highly overestimates the slope effect. The equation proposed by Atkinson and Wu underestimates the slope effect to some extent, probably due to the water spray cooling applied in their tests. The equation proposed by Chow et al. gives reasonably good prediction of the slope effect. Note that Weng et al.'s experimental data show a much more significant influence of slope on critical velocity but their CFD results for tunnels with aspect ratio (AR) greater than one show similar results as the test data obtained in this work.
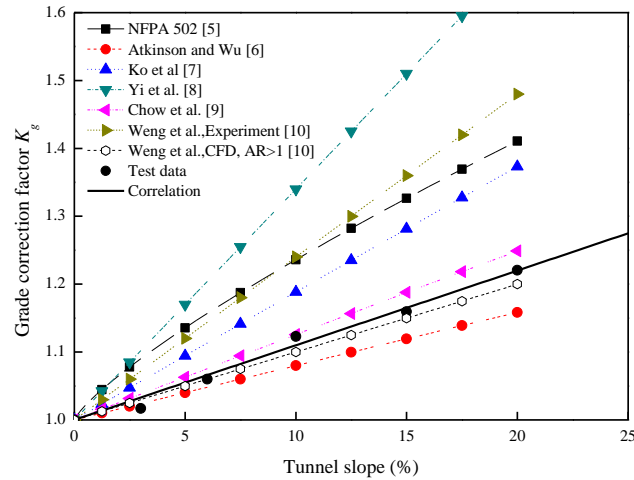
Figure 21. Comparison of the tests data with others' correlations for grade factor K_g.

7.3 Backlayering length for downhill tunnels

7.3.1 Influence of fire size and slope

The backlayering lengths for various heat release rates as a function of velocity are shown in Figure 22 for 0 % slope and Figure 23 for 20 % slope. For a given velocity, the backlayering length increases with the heat release rate below 20 kW, while becomes less sensitive above 20 kW, similar to the previous findings [2010]. Comparing the two figures shows that, for a given velocity and heat release rate, the backlayering length for 20 % is systematically larger, indicating a greater critical velocity. Further, the backlayering length decreases with the increasing velocity as expected.
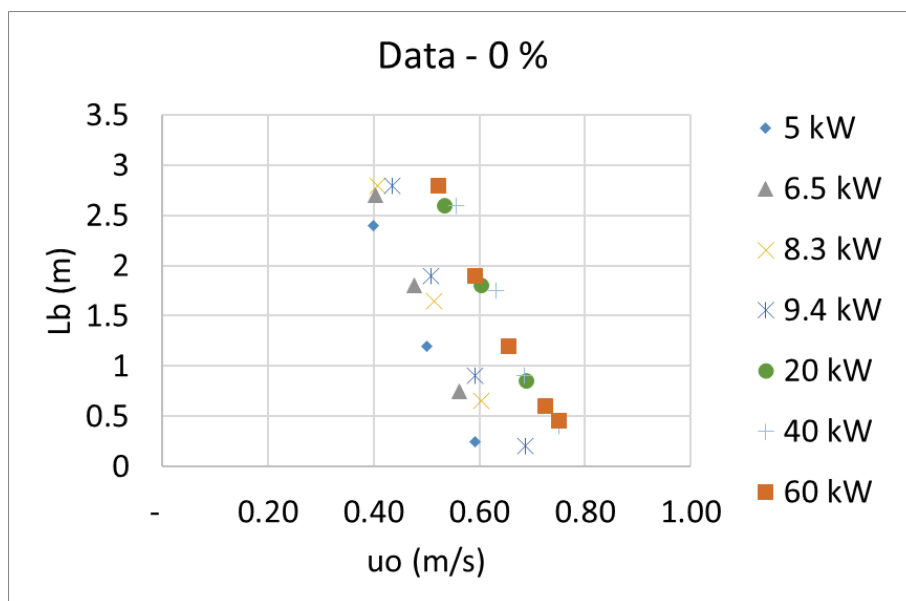
Figure 22. Backlayering length vs. tunnel velocity for 0 % slope.
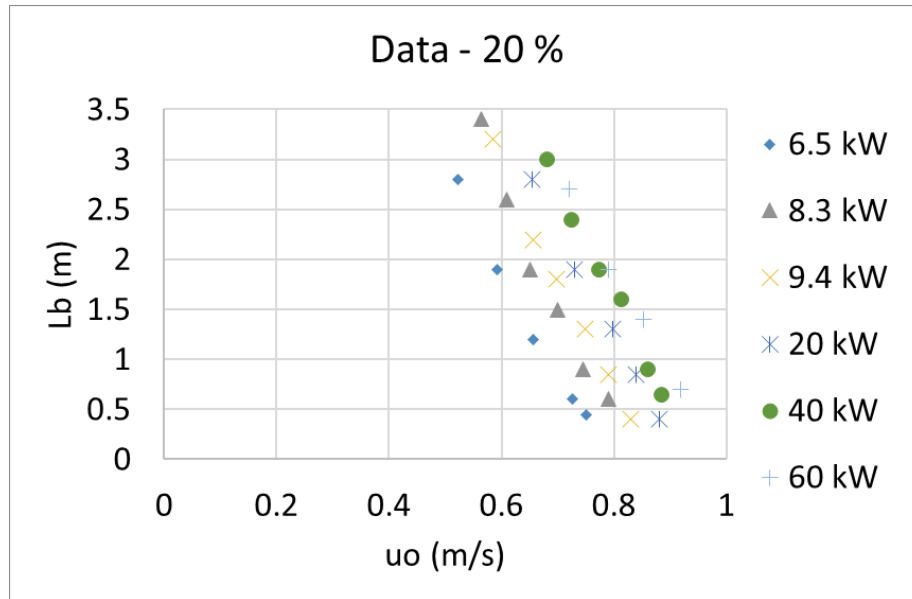
Figure 23. Backlayering length vs. tunnel velocity for 20 % slope.

7.3.2 Correlation for backlayering length

All the data for backlayering length are plotted in non-dimension form in Figure 24. The data for backlayering length with various slopes obtained in this study comply Eq. (2) reasonably well:

$$L_b^* = \frac{L_b}{H} = 18.5 \ln(u_c / u_o) \tag{2}$$
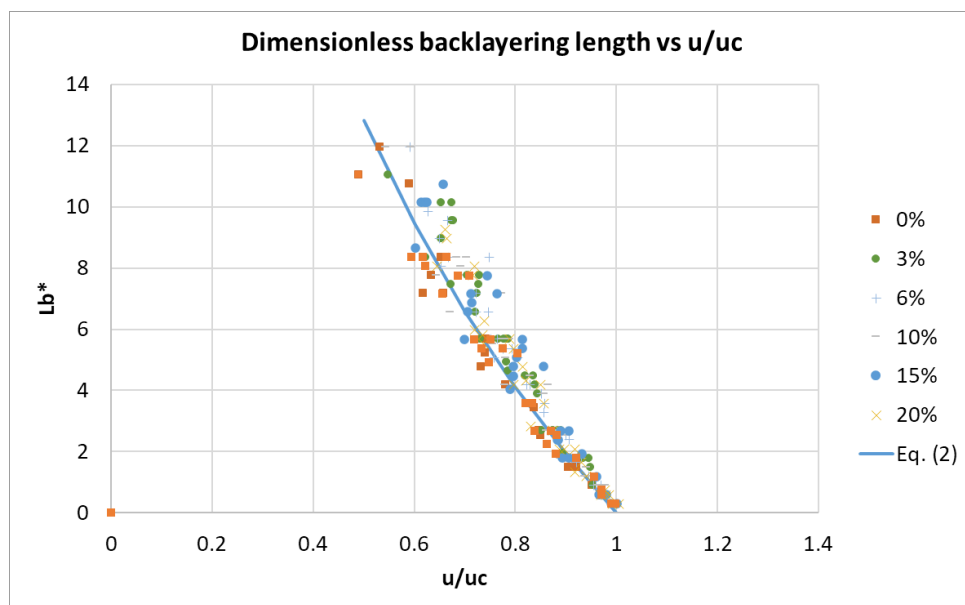
Figure 24. Dimensionless backlayering length vs. dimensionless tunnel velocity.

Although Eq. (2) give reasonably good estimations of the backlayering length, the data lie between -19 % and 35 % of the predictions, as shown in Figure 25. Therefore, to make a conservative estimation of the backlayering length, the following equation may be used:

$$L_b^* = \frac{L_b}{H} = 25\ln(u_c / u_o) \tag{4}$$

which refer to the upper range in Figure 25. Note that the lower range refers to a constant of 15, in comparison to 25 in Eq. (4).
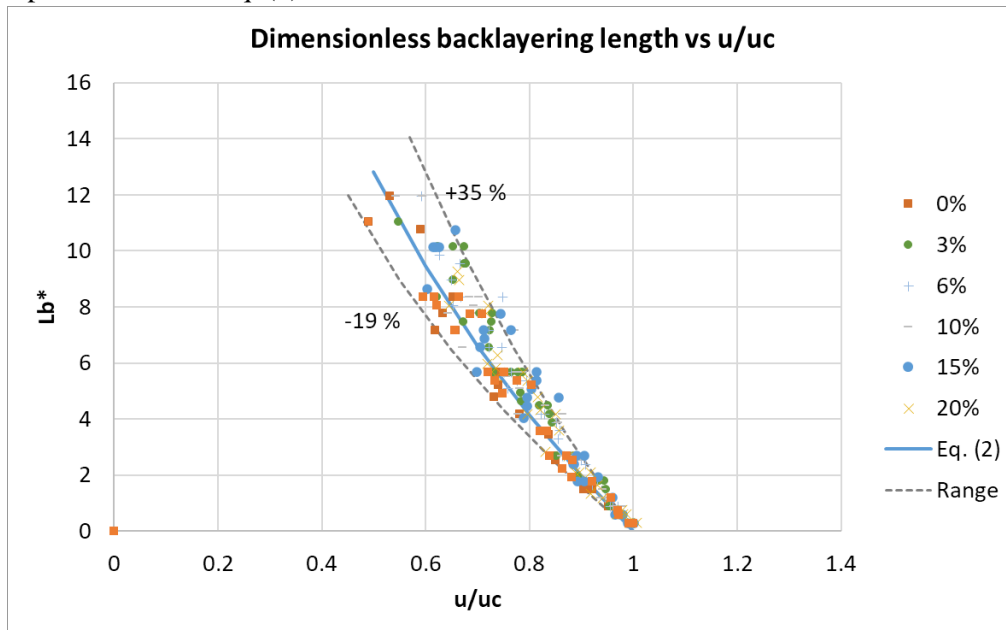
Figure 25. Dimensionless backlayering length vs. dimensionless tunnel velocity.

8   Experimental results and analysis – Uphill tunnels

8.1   Critical velocity for uphill tunnels

The data for critical velocity ratio (grade correction factor) is plotted as a function of tunnel slope for 9.4 kW and 40 kW in Figure 26. The test data clearly show that the critical velocity for an uphill tunnel becomes less than that for a horizontal tunnel. The critical velocity ratio is also not sensitive to the heat release rate, and it may also be expressed as a linear function of the slope.
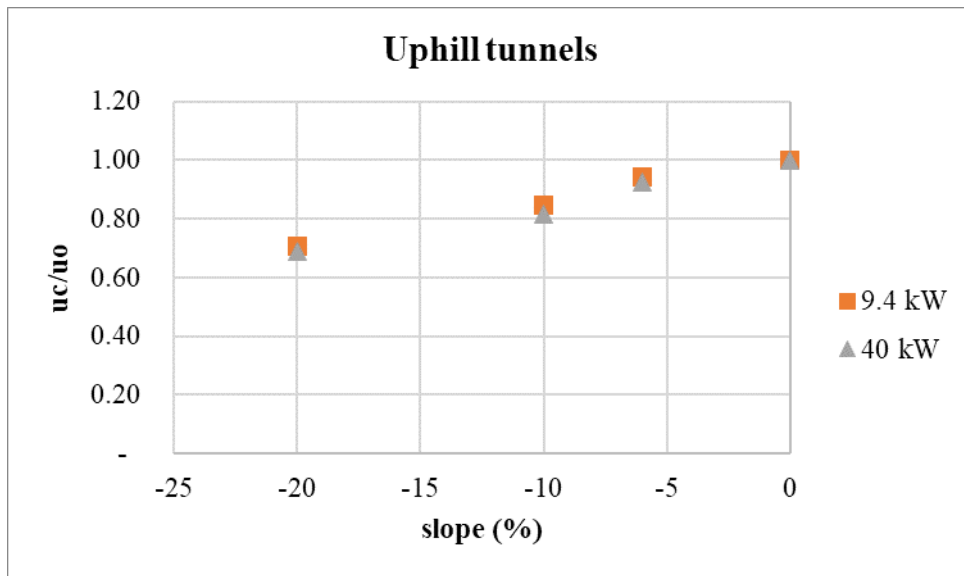
Figure 26. Dimensionless critical velocity vs slope for 9.4 kW and 40 kW.

For each slope, the data for various heat release rates tested are averaged, and plotted in Figure 20. It can be seen that the averaged data are well correlated with the following linear correlation:

$$\frac{u_c}{u_c(0)} = 1 + 0.015\,s \tag{5}$$

where s is tunnel slope in %. The above equation indicates that if a tunnel has an uphill slope of 10 %, the critical velocity will be reduced by 15 % in comparison to the corresponding horizontal tunnel.

Compared Eq. (5) for uphill tunnels with Eq. (3) for downhill tunnels indicates that the slope for an uphill tunnel seems to have a more obvious effect on critical velocity, although the difference is not so significant.
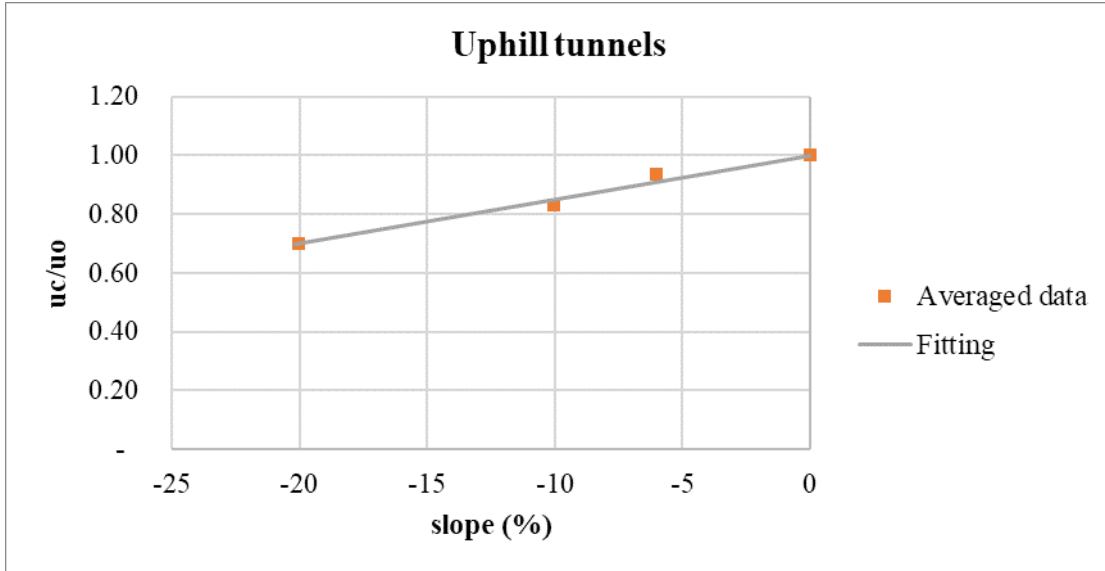
Figure 27. Correlation for critical velocity ratio vs uphill slope.

8.2   Backlayeringlength for uphill tunnels

The backlayeirng lengths for 10 kW with slopes of 0 % and -6 % are compared in Figure 28. It can be found that the results for backlayeirng length in uphill tunnels show quite different variations with the velocity, in comparison to the horizontal tunnels. The variation of backlayeirng length is much smaller for the -6 % slope. This indicates that the predictions using Eq. (2) give conservative results for backlayering lengths in uphill tunnels.
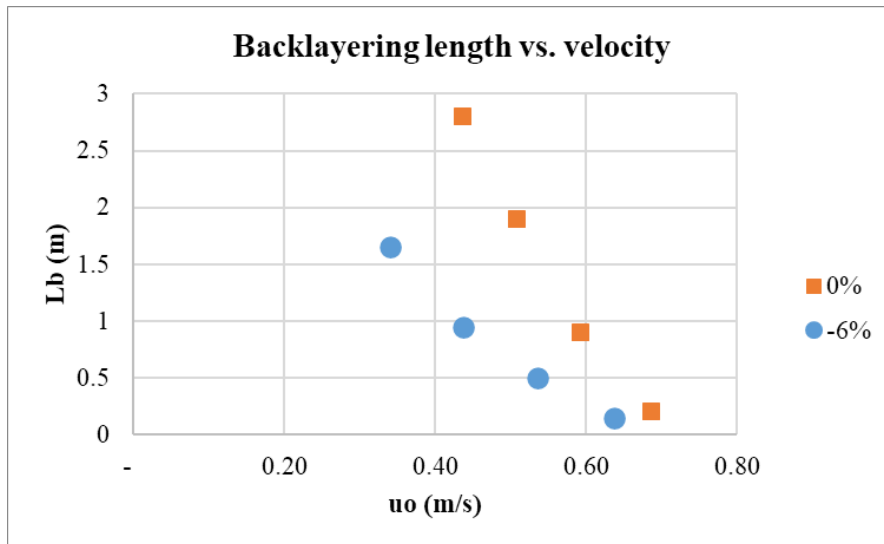
Figure 28. Comparison of backlayering length for various slopes at 10 kW.

This phenomenon can be observed more clearly when the velocity becomes 0m/s, seeing Figure 29. There appears to be an upper limit for the backlayering length in an uphill tunnel. This value is measured to lie between 1.6 m and 1.7 m for the 20 % uphill tunnel at 10 kW, and it is 1.7 m at 40 kW. Therefore, this upper limit is insensitive to the heat release rate. A simple correlation could be used to estimate this upper limit:

$$L_{b,\max} = \frac{H_{ef}}{|s|} \tag{6}$$

where H_{ef} is the ceiling height above the bottom of the fire source, i.e. the distance between the bottom of the fire source and the ceiling at a tunnel cross section. If the fire source is on the floor, H_{ef} quals tunnel height H.

The above correlation refers to the scenario that the bottom of the backlayering layer is at the same height as the bottom of the fire source.

It can be found that the backlayering length is rather insensitive to the variation of the ventilation velocity for a slope as great as 20 %. In other words, in such a case, a great change in velocity only results in minor change in the backlayering length. This indicates that increasing the tunnel velocity is not so beneficial in terms of reducing backlayering length in an uphill tunnel. Also note that the upper limits for backlayering length exist. This means that for a large uphill slope, even if the velocity is much lower than the critical velocity, the backlayering length is quite short and tolerable. The objectives of smoke control for uphill tunnels with a great slope may thus vary, i.e. a lower ventilation capacity is required for smoke control.

Figure 29. Backlayering length for 20 % at 10 kW.

9 Numerical simulations

CFD modelling (Computational Fluid Dynamics) is a good complement to model scale and large scale testing. Changes of tunnel g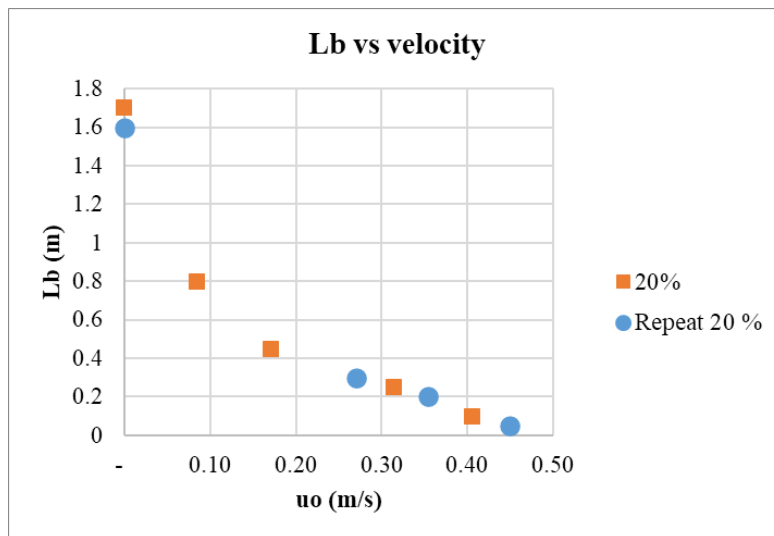eometry, fire size and other installation conditions are much easier and more cost effective in CFD modelling compared to model or full scale testing.

Fire Dynamics Simulator (FDS 6.2.0) was applied in this work [21]. Large Eddy Simulation was chosen for modelling of turbulence related to the fire flows.

CFD modelling is conducted to investigate the influence of slope on critical velocity in both downhill and uphill tunnels. But at first a verification of modelling is conducted based on the model scale data obtained, including grid sensitivity analyses.

9.1 Verification of modelling

9.1.1 Grid sensitivity analysis

Grid sensitivity analyses are conducted for both model scale tunnel and full scale tunnel. Grid cell size is a key issue related to both computation time cost and accuracy. For fire modeling, the fire region attracts our special attention. Note that the flame properties are directly related to the fire characteristic diameter, which can be expressed as follows [21]:

$$D^* = (\frac{Q}{\rho_o c_p T_o \sqrt{g}})^{2/5} \tag{1}$$

where Q is heat release rate (HRR, kW) and D^* is the fire characteristic diameter (m). Note that the characteristic diameter D^* is directly related to the HRR. Generally a cell size of $0.075D^*$ to $0.1D^*$ is reasonable value for modelling of tunnel fires [22]. It should be kept in mind that for modelling of tunnel fires, the restrictions of tunnel structure also affects the grid size required for CFD modelling. For example, the grid size needs to be fine so as to model the flow and heat transfer for the ceiling jets.

Note that a smaller fire corresponds to a smaller cell size based on the above analysis. In a model scale fire, the grid size is much smaller than that in full scale. For a tunnel with a height of H, Eq. (1) can be transformed into [22].

$$\frac{D^*}{H} = (\frac{Q}{\rho_0 c_p T_o g^{1/2} H^{5/2}})^{2/5} = Q^{*2/5} \tag{2}$$

This means that at the same dimensionless HRR, the fire characteristic diameter is directly related to the tunnel height, i.e. the reasonable mesh size is proportional to the tunnel height. This also means that the ratio of reasonable mesh sizes between model scale and full scale equals the scale ratio. In other words, the grid numbers required for model scale and full scale is about the same.

Note that this conclusion is deduced based on a similar flow mode and the same dimensionless HRR.

In this work, a grid sensitivity analysis is conducted before verification of numerical modelling. The simulated model scale tunnel has the same tunnel cross section and materials as in the tests, with a total length of 7 m (4.5 m upstream and 2.5 m downstream). Two cases are studied, i.e. Case 1 with 0 % slope and 0.54 m/s and Case 2 with 20% downhill slope and 0.64 m/s. The heat release rate is 6.5 kW. The simulation time is 100 seconds, corresponding to around 6.5 min in full scale. Three grid sizes are chosen for the grid analysis, i.e. around 0.013 m (Grid system A), 0.02 m (Grid system B) and 0.033 m (Grid system C). In other words, the grid size is in a range of 0.1 D* to 0.26 D*.

Comparisons of results for various grid sizes are given in Table 4 for the two cases. As shown in Table 4, when the grid size decreases to a value around 0.02 m, the influence of grid size on the smoke backlayering length, L_b, becomes limited in both cases. In the verification of modelling, the grid size of 0.013 m (Grid system A) is used.

Table 4. Comparisons of results for grid sensitivity analysis in the two cases.

Grid system	Gridding (*L×W×H*)	L_b (m) for Case 1: 0 % slope, 6.5 kW, 0.54 m/s	L_b (m) for Case 2: 20 % slope, 6.5 kW, 0.64 m/s
A	526×39×25	0.5	0.4
B	350×26×20	0.45	0.35
C	212×16×10	0.05	0

9.1.2 Verification of modelling against tests

In the following, a total of 4 tests were simulated, including tests with fire sizes of 6.5 kW and 60 kW with slopes of 0 % and 20 %. The results are compared with the test data for verification of the modelling.

The numerical results for critical velocity are compared with values obtained from these tests, see Table 5. The results agree well. The difference is within 2 % for the simulated cases.

Table 5. Comparisons of test data and simulation results.

Test no.	Q (kW)	Slope	uc (m/s)		Difference
			test	simulation	
102	6.5	0%	0.65	0.64	-1.8%
601	6.5	20%	0.77	0.78	1.3%
107	60	0%	0.79	0.80	1.7%
606	60	20%	1.00	0.99	-0.7%

The numerical results for backlayering length are also compared with values obtained from these tests, seeing Figure 30 for 6.5 kW and Figure 31 for 60 kW. Overall, a reasonably good agreement

can be found. But it can also be found that, for scenarios with 20 % slope, the simulated backlayering length is less sensitive to velocity, compared to the test data, especially for the case with 6.5 kW. This may indicate that a larger discrepancy is expected in case of a long backlayering length while simulating a sloped tunnel.
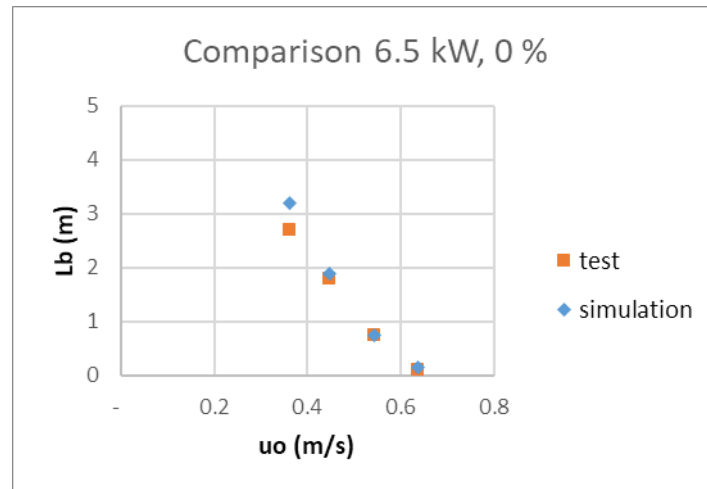
(a) 6.5 kW, 0 %
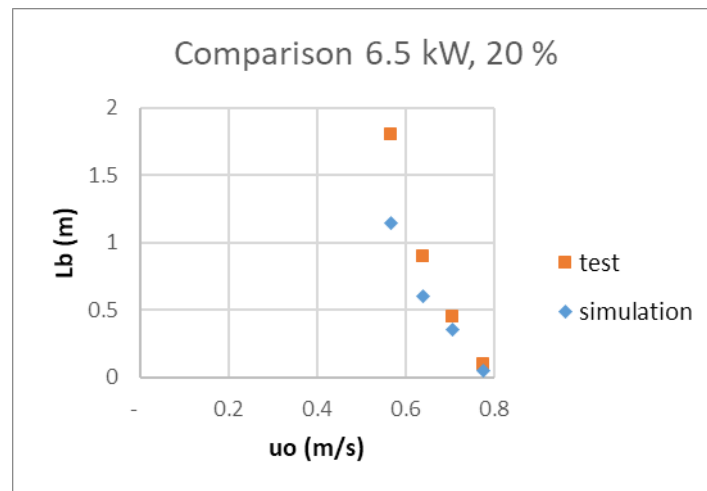
(a) 6.5 kW, 20 %

Figure 30. Comparison of backlayering length between test and simulation for 6.5 kW.
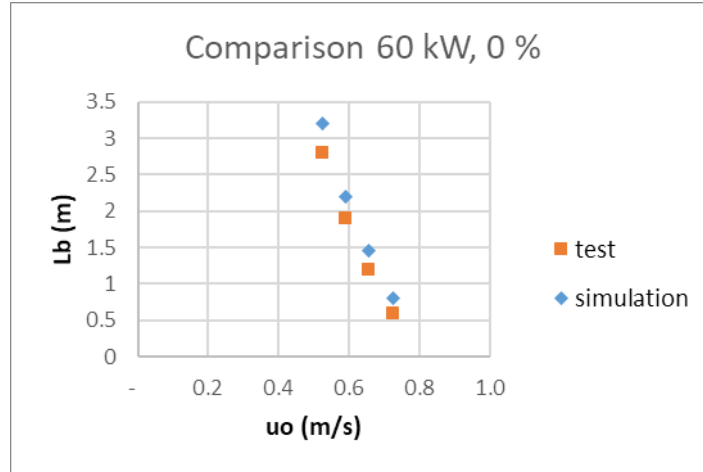
(a) 60 kW, 0 %
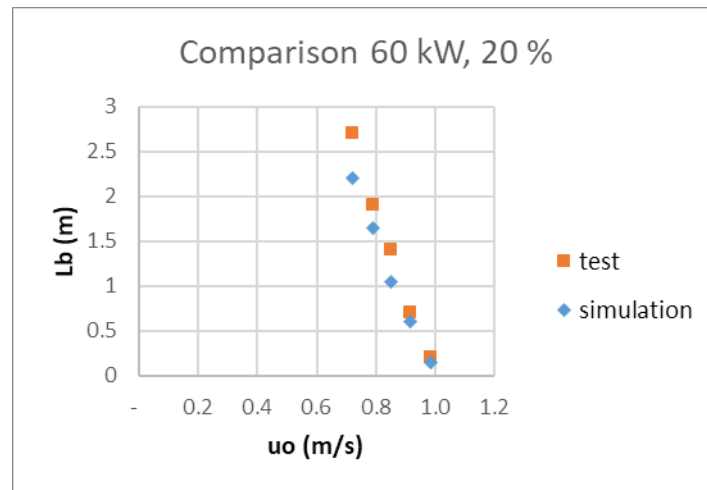
(a) 60 kW, 20 %

Figure 31. Comparison of backlayering length between test and simulation for 60 kW.

9.2 Simulation scenarios

The simulated tunnel is 100 m long with the fire placed on the floor at the center of the tunnel. The fire source is assumed to have combustion properties similar to heptane. The focus of the study is on the influence of slope on the critical velocity, both for downhill and uphill tunnels.

9.2.1 Grid sensitivity analysis

A grid sensitivity study is conducted before simulating the scenarios of interest in this study. Two cases are studied, i.e. Case 1 with 0 % slope and 2.0 m/s and Case 2 with 20% downhill slope and 2.3 m/s. The heat release rate is 5.7 MW. The simulation time is 200 seconds. Three grid sizes are chosen for the grid analysis, i.e. around 0.2 m (Grid system A), 0.3m (Grid system B) and 0.5 m (Grid system C). In other words, the grid size is in a range of 0.1 D* to 0.26 D*.

Comparisons of results for various grid sizes are given in Table 6 for the two cases. As shown in Table 6, when the grid size decreases to a value around 0.3 m, the influence of grid size on the smoke backlayering length, L_b, becomes limited in both cases. In the verification of modelling, the grid size of 0.2 m (Grid system A) is used.

Table 6. Comparisons of results for grid sensitivity analysis in the two cases.

Grid system	*Gridding (L×W×H)*	L_b (m) for Case 1: 0 % slope, 5.7 MW, 2 m/s	L_b (m) for Case 2: 20 % slope, 5.7 MW, 2.3 m/s
A	500×39×25	8	6
B	333×26×20	9	6
C	200×16×10	2	0

9.2.2   Scenarios

The simulation scenarios for downhill slopes are listed in Table 7. Two tunnel cross sections were simulated, both having a height of 5 m but a different width (7.8 m or 15 m). Two fire size were investigated, i.e. 5.7 MW and 52.3 MW, and four downhill slopes were studied, i.e. 0 %, 5%, 10 % and 20 %. The gridding is 500×39×25 for the 7.8 m wide tunnel while it is 500×75×25 for the 15 m wide tunnel.

Table 7. List of simulations with downhill slopes.

Case No.	Tunnel H(m)*W(m)	HRR (MW)	Slope (%)	u (m/s)
1	5×7.8	5.7	0	1.81,1.93,2.03,2.23
2	5×7.8	5.7	5	1.89,2.01,2.15,2.33
3	5×7.8	5.7	10	1.97,2.10,2.24,2.43
4	5×7.8	5.7	20	2.14,2.27,2.43,2.63
5	5×7.8	52.3	0	2.4,2.56,2.73,2.96
6	5×7.8	52.3	5	2.51,2.67,2.85,3.10
7	5×7.8	52.3	10	2.62,2.79,2.98,3.23
8	5×7.8	52.3	20	2.83,3.02,3.22,3.50
9	5×15	5.7	0	1.71,1.82,1.95,2.11
10	5×15	5.7	5	1.79,1.91,2.03,2.21
11	5×15	5.7	10	1.87,1.99,2.12,2.30
12	5×15	5.7	20	2.2,2.15,2.30,2.49
13	5×15	52.3	0	2.4,2.56,2.73,2.96
14	5×15	52.3	5	2.51,2.67,2.85,3.10
15	5×15	52.3	10	2.62,2.79,2.98,3.23
16	5×15	52.3	20	2.83,3.02,3.22,3.50

The simulation scenarios for uphill slopes are listed in Table 8. The tunnel studied has a height of 5 m and a width of 7.8 m. The fire size is 5.7 MW. Four uphill slopes were studied, i.e. 0 %, 5%, 10 % and 20 %.

Table 8. List of simulations with uphill slopes.

Case No.	Tunnel H(m)*W(m)	HRR (MW)	Slope (%)	u (m/s)
1	5×7.8	5.7	0	1.81,1.93,2.03,2.23
2	5×7.8	5.7	5	1.71,1.82,1.94,2.11
3	5×7.8	5.7	10	1.25,1.46,1.67,1.88
4	5×7.8	5.7	20	0,0.92,1.37,1.65

9.3 Downhill tunnels

The results for critical velocities are summarized in Table 9. The obtained critical velocities for 0 % slope are close to the values obtained by Eq. (1). The influence of slope is plotted in Figure 32, together with the proposed correlation based on model scale test data obtained in this study, Eq. (3). It can be seen that the results comply the correlation well for both tunnel cross sections and both fire sizes.

Table 9. Summary of critical velocities with downhill slopes.

Case No.	Tunnel H(m)*W(m)	HRR (MW)	Slope (%)	u_c (m/s)
1	5×7.8	5.7	0	2.25
2	5×7.8	5.7	5	2.39
3	5×7.8	5.7	10	2.48
4	5×7.8	5.7	20	2.66
5	5×7.8	52.3	0	3.04
6	5×7.8	52.3	5	3.21
7	5×7.8	52.3	10	3.45
8	5×7.8	52.3	20	3.73
9	5×15	5.7	0	2.13
10	5×15	5.7	5	2.22
11	5×15	5.7	10	2.35
12	5×15	5.7	20	2.58
13	5×15	52.3	0	3.21
14	5×15	52.3	5	3.46
15	5×15	52.3	10	3.60
16	5×15	52.3	20	3.84
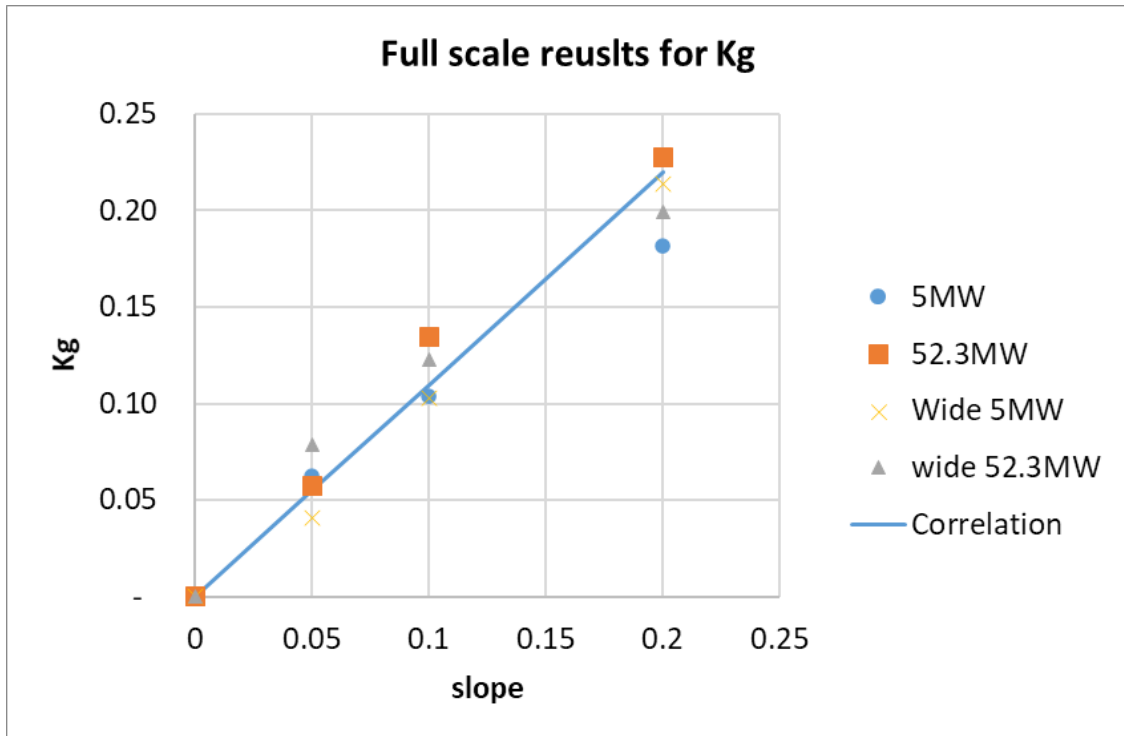
Figure 32. Full scale results of Kg vs downhill slope.

9.4   Uphill tunnels

The smoke distribution is shown in Figure 33. The fresh air flows from the left to right side. It is clearly shown that the bottom of the upstream smoke layer is horizontal, rather than parallel to the tunnel floor. The phenomenon can be more clearly observed when the ventilation velocity is 0 m/s. In such case, the smoke won't descend further as the downward movement is restrained by the buoyancy force. Downward diffusion is still possible when the smoke lose buoyancy, i.e. smoke temperature is close to ambient, but then the concentration of smoke is much less and probably not hazardous to personnel. This confirms the findings from the model scale tests.
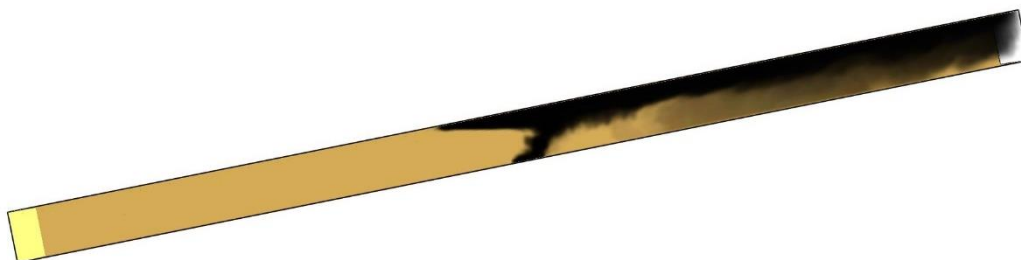
(a) u_o=0.92 m/s

(b) u_o=0 m/s

Figure 33. Smoke distribution in 20 % uphill tunnel with 0.92 m/s and 0 m/s.

The backlayering lengths for various uphill slopes are shown in Figure 34. It can be seen clearly that the backlayering length increases much more slowly with decreasing velocities for a greater slope, especially for 20 % slope. Further, the backlayeirng length for 20 % slope reaches an upper limit of 30 m when the velocity becomes 0 m/s. This confirms the findings from the model scale tests, noting that the theoretical value is estimated to be 25 m, according to Eq. (6).
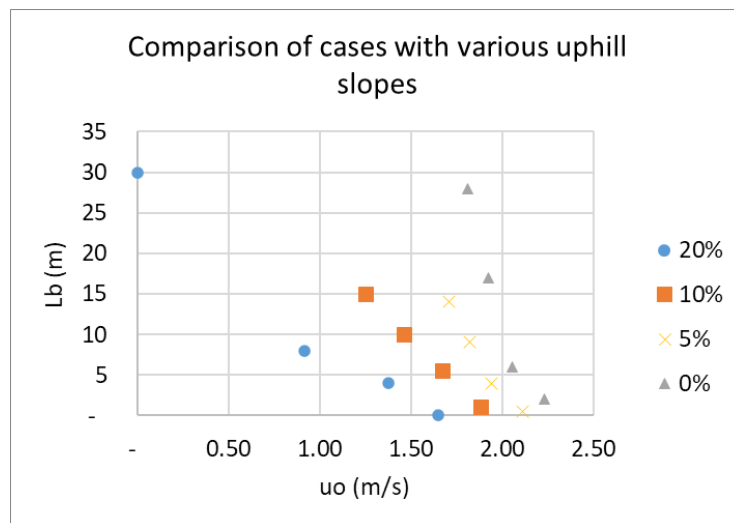
Figure 34. Backlayering length vs. velocity for various uphill slopes

The influence of uphill slope on critical velocity is plotted in Figure 35, together with the proposed correlation based on model scale test data obtained in this study, Eq. (5). It can be seen that the results comply the correlation well.

Overall, there is good agreement between the model scale tests and full scale numerical simulations for both downhill and uphill tunnels, concerning the influence of slope on smoke control.
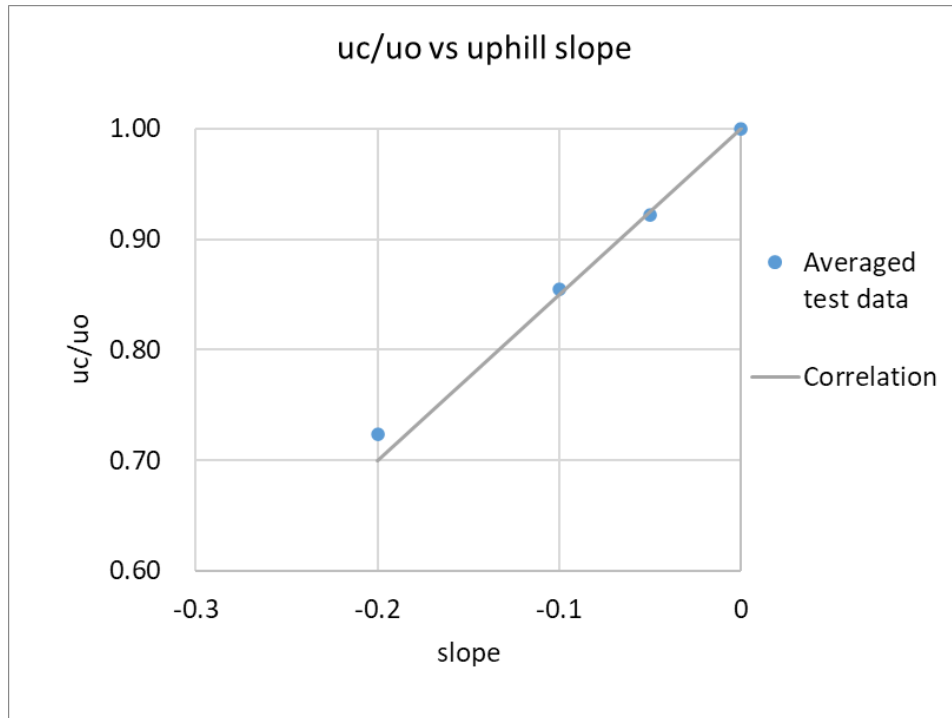
Figure 35. Full scale results of Kg vs uphill slope.

10   Conclusions

A total of 46 tests were carried out in a 1:15 model scale tunnel with various slopes to investigate the influence of downhill and uphill slopes on smoke control in longitudinally ventilated tunnels. The experimental study considered various fire sizes, from small to large fires, and various slopes, from -20 % (uphill) to 20 % (downhill). Further, a series of simulations were conducted to verify the findings in full scale tunnels. A positive slope refers to a tunnel with longitudinal flow blown towards the downhill side and vice versa.

The main findings are summarized below:

(1) Experimental data for downhill slopes ($s \geq 0$) within a range of 0 % – 20 % show that the critical velocity can be well correlated with the downhill slope by Eq. (3):

$$\frac{u_c}{u_c(0)} = 1 + 0.011\,s \tag{3}$$

where s refers to downhill slope ($s \geq 0$).

(2) Experimental data for uphill slopes ($s < 0$) within a range of -20 % -0 % show that the critical velocity can be well correlated with the uphill slope by Eq. (5):

$$\frac{u_c}{u_c(0)} = 1 + 0.015\,s \tag{5}$$

where s refers to uphill slope ($s < 0$).

(3) For an uphill tunnel ($s < 0$), the backlayering length become less sensitive to the variation of tunnel velocity, and there is an upper limit for backlayeirng length, which can be approximately estimated by the following equation:

$$L_{b,\max} = \frac{H_{ef}}{|s|} \tag{6}$$

where H_{ef} is the ceiling height above the bottom of the fire source, i.e. the distance between the bottom of the fire source and the ceiling at a tunnel cross section. If the fire source is on the floor, H_{ef} quals tunnel height H. Further, Eq. (2) give conservative results for backlayering lengths in uphill tunnels.

(4) The previous equation for critical velocity, Eq. (1), correlates well with the test data for horizontal tunnel. The previous equation for backlayeirng length, Eq. (2), correlates reasonably well with the test data for horizontal tunnel and downhill tunnels, but to make a conservative estimation of the backlayering length, a constant of 25 might be used instead of 18.5 in Eq. (2). It should be kept in mind that the backlayering length for uphill tunnels become less sensitive to the variation of tunnel velocity.

(5) Numerical simulations of full scale tunnels with various cross sections, fire sizes and slopes, confirm the above findings.

References

1. Ingason, H., A. Lönnermark, and Y.Z. Li, *Model of ventilation flows during large tunnel fires.* Tunnelling and Underground Space Technology, 2012. **30**: p. 64-73.
2. Li, Y.Z. and H. Ingason, *Overview of research on fire safety in underground road and railway tunnels.* Tunnelling and Underground Space Technology, 2018. **81**: p. 568-589.
3. Li, Y.Z., B. Lei, and H. Ingason, *Study of critical velocity and backlayering length in longitudinally ventilated tunnel fires.* Fire Safety Journal, 2010. **45**: p. 361-370.
4. Li, Y.Z. and H. Ingason, *Effect of cross section on critical velocity in longitudinally ventilated tunnel fires.* Fire Safety Journal, 2017. **91**: p. 303–311.
5. *NFPA 502 - Standard for Road Tunnels, Bridges, and Other Limited Access Highways.* 2017 Edition, National Fire Protection Association.
6. Atkinson, G.T. and Y. Wu, *Smoke Control in Sloping Tunnels.* Fire Safety Journal, 1996. **27**: p. 335-341.
7. Ko, G.H., S.R. Kim, and H.S. Ryou, *An experimental study on the effect of slope on the critical* Journal of Fire Sciences, 2010. **28**: p. 27–47.
8. Yi L., et al., *An experimental study on critical velocity in sloping tunnel with longitudinal ventilation under fire.* Tunnelling and Underground Space Technology, 2014. **43**: p. 198-203.
9. Chow W.K., et al., *Smoke movement in tilted tunnel fires with longitudinal ventilation.* Fire Safety Journal, 2015. **75**: p. 14–22.
10. Weng M.C., et al., *Study on the critical velocity in a sloping tunnel fire under longitudinal ventilation.* Applied Thermal Engineering, 2016. **94**: p. 422–434.
11. Bakke P. and Leach S. J., *Turbulent diffusion of a buoyant layer at a wall.* Appl. Sci. Res., 1965. **15**: p. 97-136.
12. Grant, G.B., S.F. Jagger, and C.J. Lea, *Fires in tunnels.* Phil. Trans. R. Soc. Lond., 1998. **356**: p. 2873-2906.
13. Li, Y.Z. and T. Hertzberg, *Scaling of internal wall temperatures in enclosure fires.* Journal of Fire Sciences, 2015. **33**(2): p. 113-141.
14. Yao, Y., et al., *Scale effect of mass loss rates for pool fires in an open environment and in tunnels with wind.* Fire Safety Journal, 2019. **105**: p. 41-50.
15. Thomas, P., *The movement of buoyant fluid against a stream and the venting of underground fires.* 1958, Fire Research Station: Boreham Wood.
16. Li, Y.Z. and H. Ingason, *The maximum ceiling gas temperature in a large tunnel fire.* Fire Safety Journal, 2012. **48**: p. 38-48.
17. Li, Y.Z. and H. Ingason, *The fire growth rate in a ventilated tunnel fire*, in *10th International Symposium on Fire Safety Science (IAFSS)*. 2011: Maryland, USA. p. 347-358.
18. Li, Y.Z., H. Ingason, and A. Lönnermark, *Fire development in different scales of train carriages*, in *11th International Symposium on Fire Safety Science*. 2014: Christchurch, New Zealand. p. 302-315.
19. Ingason, H., Y.Z. Li, and A. Lönnermark, *Tunnel Fire Dynamics*. 2015, New York: Springer.
20. Li, Y.Z., *Smoke control using point extraction systems in tunnel fires*. 2018, RISE Research Institutes of Sweden, RISE Report 2018:73: Borås.
21. McGrattan, K., et al., *Fire Dynamics Simulator User's Guide (Version 6)* 2015, National Institute of Standards and Technology: USA.
22. Li, Y.Z., B. Lei, and H. Ingason, *Scale modeling and numerical simulation of smoke control for rescue stations in long railway tunnels.* Journal of Fire Protection Engineering, 2012. **22**(2): p. 101-131.

Appendix A – Numbering of instruments

Table A1. Numbering of measuremnts in the tests.

Number	Location, x	Locatoin or height above floor, z (m)	Pile	Measurement
1	-0.1	30 mm below Ceiling		TC
2	-0.2	Ceiling		TC
3	-0.3	Ceiling		TC
4	-0.4	Ceiling		TC
5	-0.5	Ceiling		TC
6	-0.6	Ceiling		TC
7	-0.7	Ceiling		TC
8	-0.8	Ceiling		TC
9	-0.9	Ceiling		TC
10	-1	Ceiling	A	TC
11	-1.1	Ceiling		TC
12	-1.2	Ceiling		TC
13	-1.3	Ceiling		TC
14	-1.4	Ceiling		TC
15	-1.5	Ceiling		TC
16	-1.6	Ceiling		TC
17	-1.7	Ceiling		TC
18	-1.8	Ceiling		TC
19	-1.9	Ceiling		TC
20	-2	Ceiling	B	TC

21	-2.2	Ceiling		TC
22	-2.4	Ceiling		TC
23	-2.6	Ceiling		TC
24	-2.8	Ceiling		TC
25	-3	Ceiling		TC
26	-3.2	Ceiling		TC
27	-3.4	Ceiling		TC
28	-3.6	Ceiling		TC
29	-3.8	Ceiling		TC
30	-4	Ceiling		TC
31	-4.4	Ceiling		TC
32	-4.8	Ceiling		TC
33	-5.2	Ceiling		TC
34	-5.6	Ceiling		TC
35	-6	Ceiling		TC
36	0	Ceiling		TC
37	0.1	Ceiling		TC
38	0.2	Ceiling		TC
39	0.3	Ceiling		TC
40	0.4	Ceiling		TC
41	0.5	Ceiling		TC
42	0.6	Ceiling		TC
43	0.7	Ceiling		TC
44	0.8	Ceiling		TC

45	1	Ceiling		TC
46	1.4	Ceiling		TC
47	1.8	Ceiling		TC
48	2.2	Ceiling		TC
49	-1	0.230	A	TC Tree
50	-1	0.165	A	TC Tree
51	-1	0.100	A	TC Tree
52	-1	0.030	A	TC Tree
20	-2	0.3	B	TC Tree
53	-2	0.23	B	TC Tree
54	-2	0.165	B	TC Tree
55	-2	0.1	B	TC Tree
56	-2	0.03	B	TC Tree
57	-4.4	0.265	D	TC Tree
58	-4.4	0.165	D	TC Tree
59	-4.4	0.065	D	TC Tree
60	1.8	0.265	E	TC Tree
61	1.8	0.165	E	TC Tree
62	1.8	0.065	E	TC Tree
63	-1	Ceiling	A	Velocity, BP
64	-2	Ceiling	B	Velocity, BP
65	-3	Ceiling	C	Velocity, BP
66	-4.4	0.265	D	Velocity, BP
67	-4.4	0.165	D	Velocity, BP

68	-4.4	0.065	D	Velocity, BP
69	1.8	0.265	E	Velocity, BP
70	1.8	0.165	E	Velocity, BP
71	1.8	0.065	E	Velocity, BP
72-74	-1	ceiling	A	Gas analysis
75-77	-2	ceiling	B	Gas analysis
78-80	-3	ceiling	C	Gas analysis

Through our international collaboration programmes with academia, industry, and the public sector, we ensure the competitiveness of the Swedish business community on an international level and contribute to a sustainable society. Our 2,200 employees support and promote all manner of innovative processes, and our roughly 100 testbeds and demonstration facilities are instrumental in developing the future-proofing of products, technologies, and services. RISE Research Institutes of Sweden is fully owned by the Swedish state.

I internationell samverkan med akademi, näringsliv och offentlig sektor bidrar vi till ett konkurrenskraftigt näringsliv och ett hållbart samhälle. RISE 2 200 medarbetare driver och stöder alla typer av innovationsprocesser. Vi erbjuder ett 100-tal test- och demonstrationsmiljöer för framtidssäkra produkter, tekniker och tjänster. RISE Research Institutes of Sweden ägs av svenska staten.